FUNDAMENTALS OF ROTOR-BEARING DYNAMICS Using *DyRoBeS*

The Jeffcott Rotor

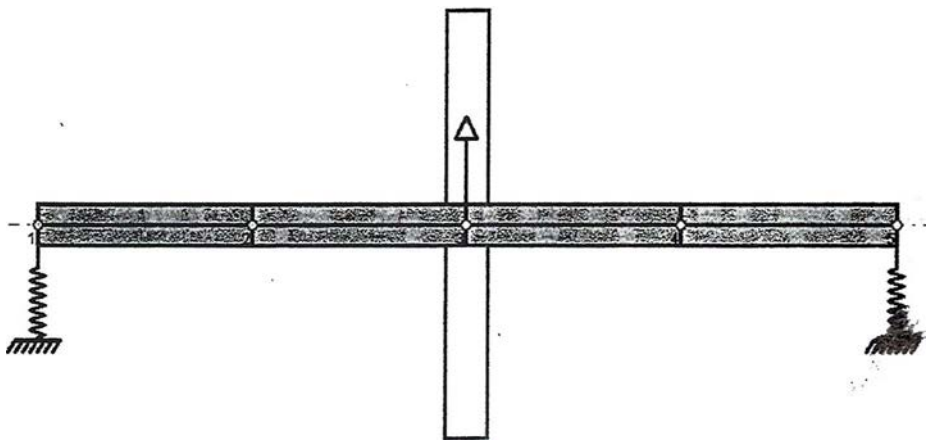

June 2002

By

Edgar J. Gunter, Ph.D.

Fellow ASME

RODYN Vibration Analysis, Inc.
1932 Arlington Boulevard
Suite 223
Charlottesville, VA 22903-1560

Phone: (434) 296-3175
Fax: (434) 971-2695
E-Mail: DrGunter@aol.com

1 INTRODUCTION TO ROTOR DYNAMICS

In this presentation, the dynamical characteristics of the basic Jeffcott rotor are addressed. The single-mass Jeffcott rotor was first addressed by H. H. Jeffcott in 1919. The study of the dynamical characteristics of the Jeffcott rotor is the starting point for the fundamentals of flexible rotor-bearing dynamics. With this model, it was now possible to explain how a rotor could pass through a critical speed.

The Jeffcott rotor is a single disk symmetrically mounted on a uniform elastic shaft. In the analysis of the original Jeffcott rotor, flexible or fluid film bearings were not considered. The rotor bearing supports are assumed to be simple pinned end conditions. The unbalance response of the Jeffcott rotor has been described by two second order differential equations to describe the dynamical motion of the system.

In Section 2, the Jeffcott rotor is analyzed using ***DyRoBeS***. The critical speeds, unbalance response, and transient motion of the Jeffcott rotor is evaluated. An extension is made of the Jeffcott rotor in this section in which shaft bow is included, as well as unbalance. There have been a number of authors such as Kramer, *Dymamics of Rotors and Foundations*, who have considered the higher modes of the Jeffcott rotor, including the gyroscopic effects of the disk. The gyroscopic effects of the Jeffcott rotor will not be considered in this section, since it has a secondary influence for a centrally mounted disk.

The self-excited instability of the Jeffcott rotor may be determined by the application of internal friction or aerodynamic Alford type of cross-coupling components acting at the rotor center. The analysis of the Jeffcott rotor is very useful, as the computer solutions may be compared to the analytic predictions.

The behavior of a multi-stage compressor or turbine through its first mode is very similar to that of a Jeffcott rotor. By means of a critical speed analysis, a compressor or turbine may often be reduced to the equivalent of a Jeffcott rotor by the computation of the rotor modal mass and stiffness for the first mode. These properties are most useful in rapidly determining the bearing optimum properties for that particular rotor.

2 SINGLE MASS JEFFCOTT ROTOR

2.1 Description of Jeffcott Rotor

Figure 2.1 represents the single mass Jeffcott rotor mounted on simple or fixed supports. The single mass Jeffcott rotor was first analyzed in 1919 and with this basic model, the behavior of the rotor passing through the critical speed region with unbalance and damping could be explained. As the first step in evaluating the dynamics of the Jeffcott rotor, the behavior with unbalance and damping will first be evaluated. The equations of motion will be presented for the Cartesian coordinates X and Y to represent the motion of the rotor center C.

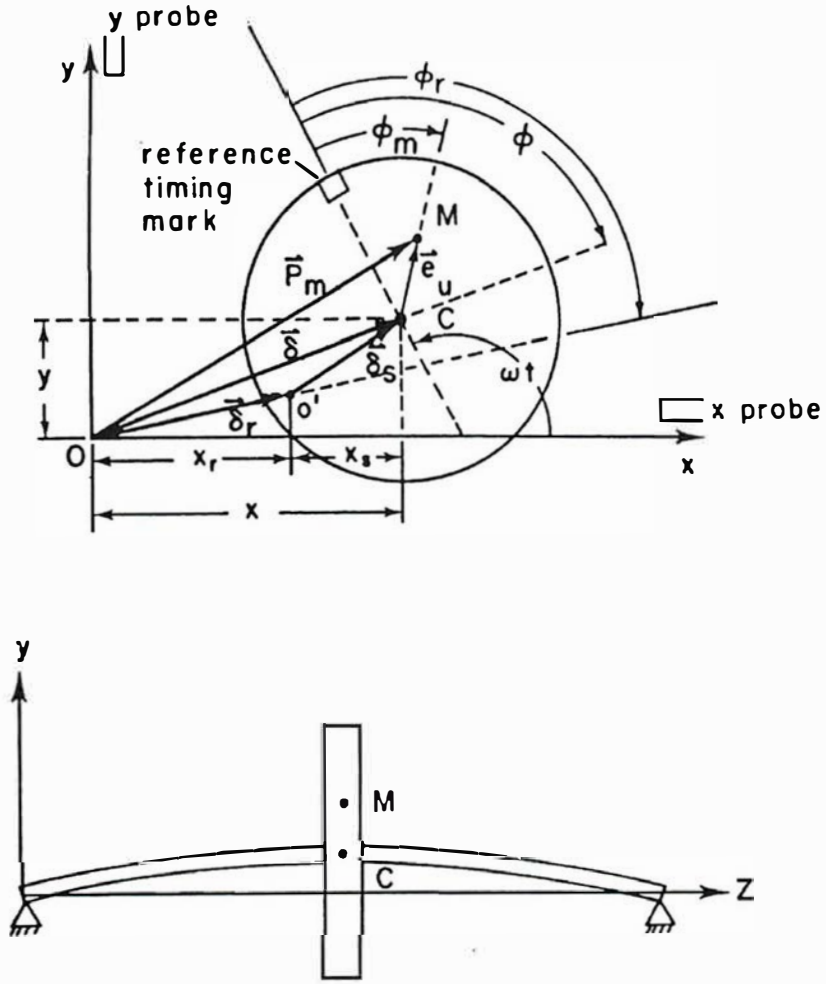

Figure 2.1 Cross Section of Jeffcott Rotor On Fixed Supports

The Jeffcott rotor is a single mass rotor mounted on a uniform elastic shaft at the center span. Normally the shaft is considered as massless and the disc has mass M. However, shaft mass may be included by placing ½ the shaft mass as lumped with the disc with no loss of accuracy. Since the disc is centered on the shaft, the gyroscopic disk moments are not included for the analysis of the rotor 1st critical speed. The bearings are considered as simple supports and provide no damping. The rotor damping is assumed to act at the shaft center.

2.2 Jeffcott Rotor Equations of Motion

The shaft mass center M is offset from the shaft elastic axis C by the distance e_u. The product of the rotor mass M times the unbalance eccentricity e_u is referred to as the rotor unbalance U_u. The rotation of the shaft at ω rad/sec causes a rotating unbalance force of magnitude

$$F_u = Me_u\omega^2 \text{, lb} \qquad (2.2\text{-}1)$$

The shaft restoring spring rate for a uniform beam simply supported is given by:

$$F_{shaft} = -K_s \times \delta_s$$
$$\text{Where } K_s = \frac{48EI}{L^3} \qquad (2.2\text{-}2)$$

There is assumed to be acting at the disk center, an external damping force. This damping force is assumed to be proportional to velocity of the disk center and is expressed as:

$$F_{damping} = -C_s \times V_c \qquad (2.2\text{-}3)$$

The damping forces oppose the motion of the shaft center. Additional forces acting at the disk center to be considered later are internal shaft friction Ci, and aerodynamic cross coupling forces Q. Both of these effects will tend to destabilize the rotor.

The 2 equations of motion in X, Y fixed coordinates for the center span shaft motion neglecting rotor acceleration are given by the following:

$$M\frac{d^2X}{dt^2} + C_s\frac{dX}{dt} + K_sX = Me_u\omega^2\cos(\omega t - \phi_m)$$
$$M\frac{d^2Y}{dt^2} + C_s\frac{dY}{dt} + K_sY = Me_u\omega^2\sin(\omega t - \phi_m) \qquad (2.2\text{-}4)$$

Undamped Motion

The equations of motion for the two degree of freedom system without damping or unbalance is equivalent to two uncoupled springs with independent motion in the x and y directions.

The equation of free vibrations in x direction, for example is of the form

$$\frac{d^2X}{dt^2} + \omega_{cr}^2X = 0$$
$$\text{Where } \omega_{cr} = \sqrt{\frac{K_s}{M_{modal}}} \qquad (2.2\text{-}5)$$

The term ω_{cr} is referred to as the rotor critical speed on rigid supports. The term M_{modal} is the rotor modal mass. If shaft mass is included as well as disk mass then the modal mass is:

$$M_{modal} = M_{disk} + \frac{M_{shaft}}{2} \qquad (2.2\text{-}6)$$

Jeffcott Rotor Station Elements

Table 2.2-1 represents the station elements of the Jeffcott rotor modeled using ***DYROBES***.

Rotor Bearing System Data

Axial Forces | Static Loads | Constraints | Misalignments | Shaft Bow | Time Forcing | Torsional/Axial
Units / Description | Material | Shaft Elements | Disks | Unbalance | Bearings | Supports | User's Elements

Shaft: 1 of 1 Starting Station #: 1 Add Shaft Del Shaft Previous Next

Speed Ratio: 1 Axial Distance: 0 Y Distance: 0

Comment: 72 IN SHAFT

	Ele	Sub	Mat	Length	Mass ID	Mass OD	Stiff ID	Stiff OD	Comments
1	1	1	1	4.500000	0.000000	6.600000	0.000000	6.600000	
2	1	2	1	4.500000	0.000000	6.600000	0.000000	6.600000	
3	1	3	1	4.500000	0.000000	6.600000	0.000000	6.600000	
4	1	4	1	4.500000	0.000000	6.600000	0.000000	6.600000	
5	2	1	1	4.500000	0.000000	6.600000	0.000000	6.600000	
6	2	2	1	4.500000	0.000000	6.600000	0.000000	6.600000	
7	2	3	1	4.500000	0.000000	6.600000	0.000000	6.600000	
8	2	4	1	4.500000	0.000000	6.600000	0.000000	6.600000	
9	3	1	1	4.500000	0.000000	6.600000	0.000000	6.600000	
10	3	2	1	4.500000	0.000000	6.600000	0.000000	6.600000	
11	3	3	1	4.500000	0.000000	6.600000	0.000000	6.600000	
12	3	4	1	4.500000	0.000000	6.600000	0.000000	6.600000	
13	4	1	1	4.500000	0.000000	6.600000	0.000000	6.600000	
14	4	2	1	4.500000	0.000000	6.600000	0.000000	6.600000	
15	4	3	1	4.500000	0.000000	6.600000	0.000000	6.600000	
16	4	4	1	4.500000	0.000000	6.600000	0.000000	6.600000	

Insert Row Delete Row Unit:(2) - Length, Diameter: in

Save Save As Close Help

Table 2.2-1 Shaft Stations of Jeffcott Rotor As A 4 Element Rotor

Table 2.2-1 shows the Jeffcott rotor modeled as a 4 element rotor. Each element is composed of 4 subelements of length 4.5 in. Masses and disks can be placed only at the major mass stations. The point of having the additional subelements is only to enhance the smoothness of the computed mode shapes.

The last station number of this model is station 5. The number of major mass stations in a model will be one greater than the number of elements. The bearings and attached disks can only be added at major mass stations. For example, the 1st bearing will be specified as acting at station 1 and the second bearing will be acting at station 5. Station 5 is automatically generated as the N+1 station number, where N is the number of elements.

Jeffcott Rotor Undamped Critical Speed Mode Shape

Fig 2.2-1 represents the undamped animated mode shape of the Jeffcott rotor on simple supports. The simulation of fixed or simple supports was made by assuming bearing stiffness values of 1.0e8 lb/in for each bearing. High values of Kb should be avoided in large models as this may lead to convergence problems caused by the creation of large matrices with stiff elements. The same principle holds for all finite element programs. In this model, a disk with a weight of 460 lb was placed at the shaft center, at station 3. If one is using the consistent unit option, then a mass of 460/386.4=1.19 would have to be specified. It is of interest to note that the 1st mode for the Jeffcott rotor could be generated with < 1% error with only a 3 station (2 element) model.

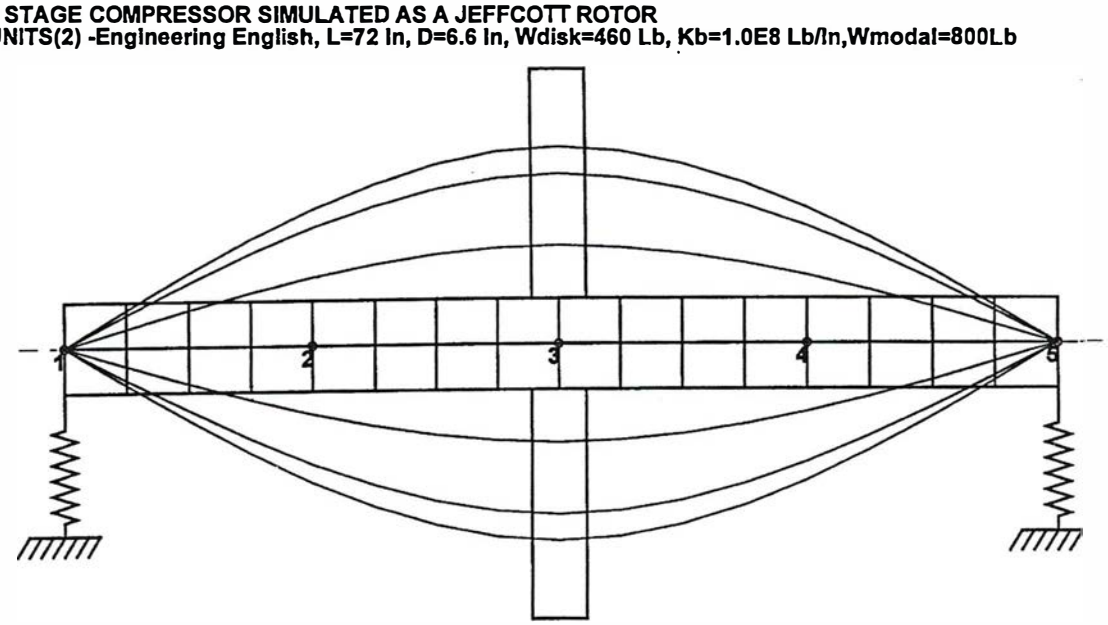

Figure 2.2-1 Jeffcott Rotor On Rigid Supports , L=72 In, D=6.6 In Wmodal=800Lb, Ncr=3,944 RPM

Fig. 2.2-1 is a representation of a Jeffcott rotor in which a 460 Lb disk is placed at the shaft center. The shaft is 72 in long with an average shaft diameter of 6.6 in. The model is a simulation of a 6 stage compressor mounted in tilting pad bearings. With the Jeffcott model we are able to determine the rotor modal properties. By knowing the rotor modal properties, we will be able to later tune the bearings or damper supports to match the modal properties of the rotor to obtain the optimum rotor damping or amplification factor.

The rotor has the following modal properties:

$$M_{modal} = 2.072,\ W_{total} = 800 Lb$$

$$K_s = 353,460\ Lb/In$$

$$\omega_{cr} = \sqrt{\frac{K_s}{M_{modal}}} = \sqrt{\frac{353,460}{2.07}} = 413\ rad/\sec = 3944\ RPM$$

The Jeffcott rotor natural frequency appears similar to a simple spring-mass system. A multistage compressor may be reduced to an equivalent Jeffcott rotor by computing the 1st critical speed and modal properties assuming stiff supports (Kb=1.0e8 lb/in). The value of Kb/Ks is almost 300. It will be demonstrated later that the optimum tuning is near unity. Thus bearing to shaft ratios >100 may be assumed to be "locked up" or rigid. The bearing damping for K ratios of Kb/Ks>10 will not be effective in the attenuation of shaft motion while passing through a critical speed. In the design of a turborotor, attention must be paid to the K ratio if the bearing damping is to be effective.

Undamped Transient Motion

The time transient motion of the rotor to an initial disturbance is given by

$$X(t) = X_o \cos(\omega_{cr} t) + \frac{V_o}{\omega_{cr}} \sin(\omega_{cr} t) \qquad (2.2\text{-}7)$$

The rotor will vibrate at its natural frequency of ω_{cr} rad/sec. The motion of the rotor in either the x or y directions is uncoupled. The motion is determined by the initial conditions of displacement and velocity.

Consider the case when the motion of the shaft acts under gravity forces only. In the case the equation of motion in the Y direction is given by:

$$\frac{d^2Y}{dt^2} + \omega_{cr}^2 Y = -g \qquad (2.2\text{-}8)$$

By knowing the natural frequency of the system, of may perform a numerical time transient analysis of the motion. One must be careful in selecting the proper time step so as to track the rotor motion. The time step is determined by the requirement to track the highest frequency in the system. In the case of the Jeffcott rotor with only one predominate frequency, an appropriate time step is determined as follows:

The rotor natural frequency is Ncr = 3,944 RPM = 65.7 CPS

$$Hz = 65.7 cps,\ \tau = 0.152 \text{sec/} cycle,\ \Delta t = 0.0015\ \ For\ 100\ steps/cycle$$

$$t_{final} = \tau_{period} \times N_{cycles} = 0.015 \times 10 = 0.15 \text{sec}$$

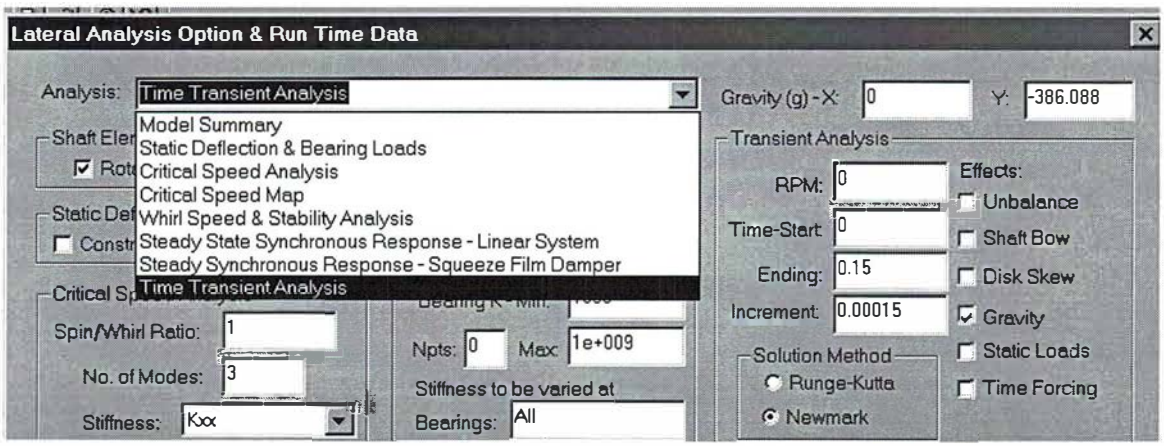

Fig 2.2-2 Time Transient Option Using Newmark Beta Integration With 100 Time Steps For 10 Cycles Of Motion

In the above Fig 2.2-3, the time transient option is selected with the only external forcing function as gravity. There is no influence due to unbalance, shaft bow, or specified external time dependent forcing functions. The use of 100 time steps per cycle is excessive. One may compute the motion with a fewer number of time steps. A similar result is achieved using the 4th order Runge-Kutta procedure. The Runge-Kutta method is self starting, and uses 4 steps per cycle. If Newmark does not start, then either the time step should be reduced or the Runge-Kutta method employed.

Fig. 2.2-3 represents the rotor transient motion under the action of gravity.

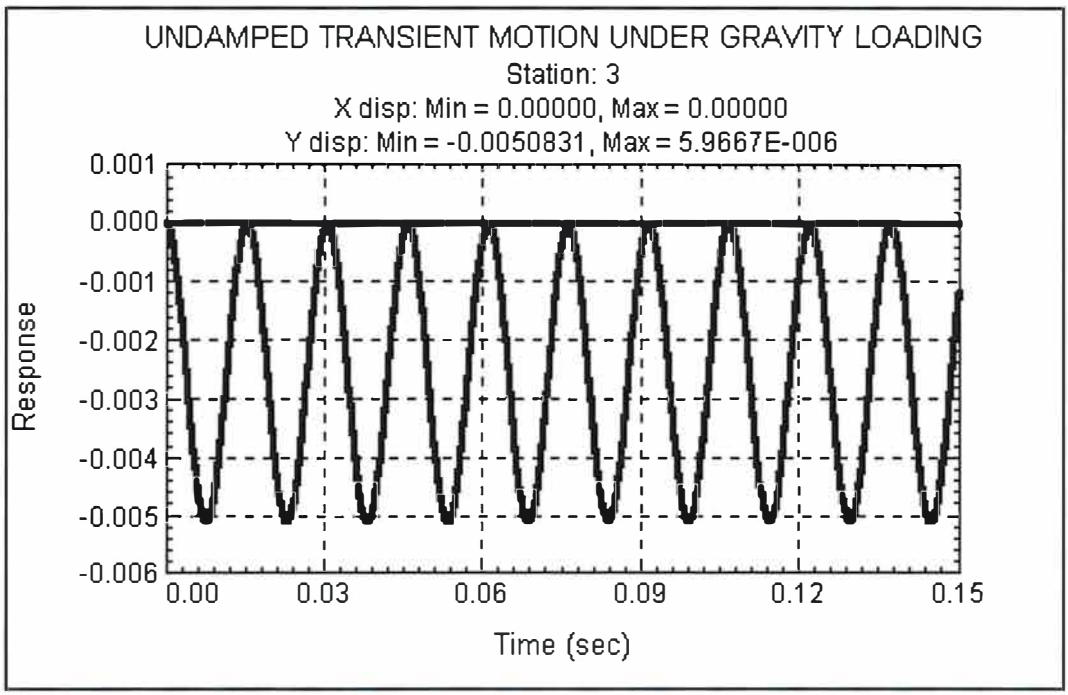

Figure 2.2-3 Time Transient Undamped Shaft Motion Under Gravity Loading For 10 Cycles of Motion

Fig 2.2-3 shows the x and y shaft motion under gravity excitation. Since the equations of motion are uncoupled, there is no horizontal motion. The vertical motion maximum displacement is twice the static displacement. The rotor continues to oscillate about the static equilibrium position. The motion is shown for 10 cycles and the frequency corresponds to the rotor natural frequency on rigid supports. For a large multistage compressor, this frequency may be determined by a simple rap test.

If the center seals are aligned with the bearing centerline, then it is seen that the rotor would be positioned at an eccentricity of 2.5 mils with respect to the seals. The static deflection of the rotor should be taken into consideration when positioning the rotor.

For a large multistage compressor, the option for static deflection should be used to determine the shaft static sag due to gravity forces. Also other external static forces may be applied to the shaft such as steam loads, gear loads, magnetic forces in order to determine the initial shaft position and corresponding static bearing loads. In a linear dynamical system, the rotor will vibrate about the static equilibrium position

In the above simple transient analysis, either the 4^{TH} order Runge-Kutta or the Newmark method will be acceptable. The Newmark method is faster but may have problems on self starting if the time step size is too large. One should determine beforehand the highest frequency that might be excited in the system. The time increment should be small enough to track the highest system frequency, ~20 steps/cycle.

2.3 Damped Transient Motion

If damping is added at the center plane of the Jeffcott rotor, then the Y equation, for example may be written in the following form(neglecting unbalance):

$$\frac{d^2Y}{dt^2} + 2\xi\omega_{cr}\frac{dY}{dt} + \omega_{cr}^2 Y = 0$$

$$Where \quad \xi = \frac{C_s}{C_c} = Damping\ Ratio \qquad (2.3\text{-}1)$$

$$C_c = 2M\omega_{cr} = Critical\ Damping$$

The transient solution for free vibrations is given by:

$$Y(t) = e^{-\xi\omega_c t}\left(\frac{V_y(0) + \xi\omega_c Y(0)}{\omega_d}\sin(\omega_d t) + Y(0)\cos(\omega_d t)\right) \qquad (2.3\text{-}2)$$

Damped Natural Frequency

When damping is added to the center of the Jeffcott rotor, the transient motion oscillates at the damped natural frequency ω_d. The motion reduces exponentially due to the influence of the damping. The damped natural frequency ω_d, for the Jeffcott rotor, is lower than the undamped natural frequency ω_c and is given by:

$$\omega_d = \omega_c\sqrt{1-\xi^2} \qquad (2.3\text{-}3)$$

Note that when the damping factor $\xi = 1$, the damped natural frequency ω_d goes to zero. The damping ratio ξ represents the ratio of rotor damping to the system critical damping.

Amplification Factor And Log Decrement

The damping ratio term ξ is not normally used in rotor dynamics. The terms that are generally employed are rotor critical speed amplification factor Ac and log decrement δ. These two terms are directly related to the damping ratio as follows:

$$A_c = \frac{1}{2\xi} = Critical\ Speed\ Amplification\ Factor \qquad (2.3\text{-}4)$$

The log decrement expressed in terms of ξ is given by:

$$\delta = \frac{2\pi\xi}{\sqrt{1-\xi^2}} = Log\ Dec \qquad (2.3\text{-}5)$$

When $\delta < 0.4$, then the approximate expression for the log decrements is:

$$\delta \cong 2\pi\xi \qquad (2.3\text{-}6)$$

Example 2.3-1 Jeffcott Rotor Damping For Ac=10

In this example, a damping acting at the rotor center will be selected to create a rotor amplification of 10. As a first step we will determine the value of critical damping Cc based on the Jeffcott rotor modal mass M and the critical speed on rigid supports ω_{cr}. For the Jeffcott rotor as shown in Sec. 2.2, the critical damping Cc is given by:

$$C_c = 2M\omega_{cr} = 2 \times 2.07 \times 413\ Rad/Sec = 1710\ Lb - Sec/In$$

For an amplification factor of 10, we have the following relationships:

$$A_c = \frac{1}{2\xi} = 10\ ;\ \xi = \frac{1}{2 \times 10} = 0.05$$

$$Cs = \xi \times C_c = 0.05 \times 1710 = 85.5\ Lb - Sec/In$$

In order to add the damping onto the rotor, an additional bearing must be placed at the rotor center, at station 3. Fig. 2.3-1 shows the rotor bearing section of ***DYROBES*** for the input of the bearing characteristics. The specification of a center span damper at station 3 is given:

$$K_{xx} = K_{yy} = 0$$

$$C_{xx} = C_{yy} = 85.8\ Lb\text{–}Sec/In$$

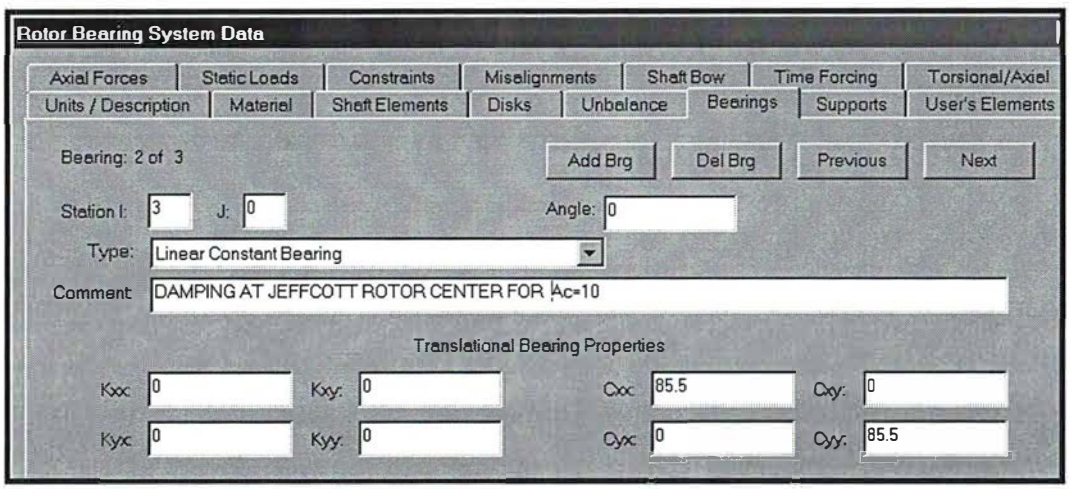

Figure 2.3-1 Center Bearing For Jeffcott Rotor For 85.5 Lb-Sec/In Damping ξ=0.05 , Ac = 10

In Fig. 2.3-1, it is seen that there are no direct bearing stiffness terms assumed. These terms would tend to increase the critical speed of the rotor. Certain types of seals may generate a direct stiffness effect, particularly water seals of pumps with a pressure differential across the seal. Later on we will add a cross coupling term Q referred to as the Alford effect such that **Q = Kxy = -Kyx**. The cross coupling effect will promote self-excited whirl instability. In this case the log dec will be negative.

Fig. 2.3-2 represents the rotor transient motion with the applied center span damping.

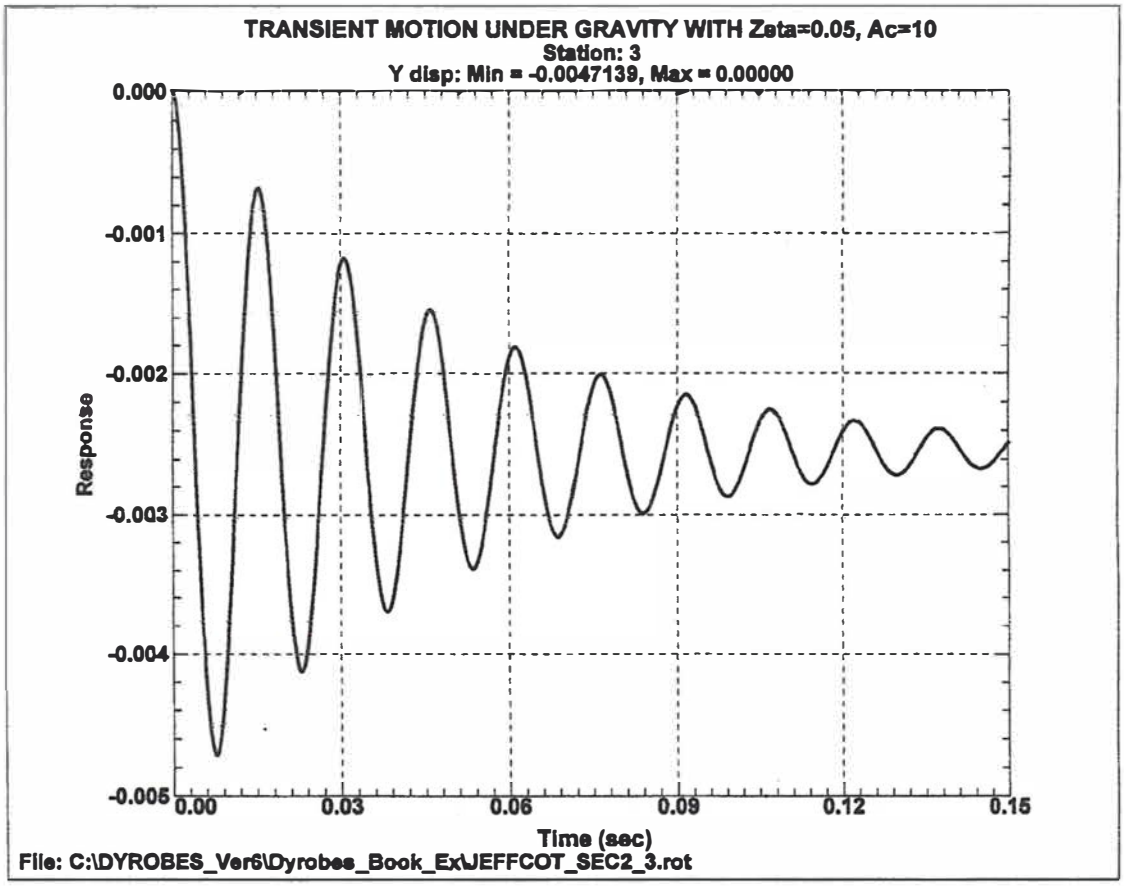

Figure 2.3-2 Damped Transient Motion of Jeffcott Rotor Under Gravity Loading With ξ=0.05 , Ac=10

The log decrement is defined as the natural logarithm of the ratio of any two successive amplitudes. The log decrement expression based on the single degree of freedom system is as follows:

$$\delta = \ln\frac{Y_1}{Y_2} = \ln\frac{e^{-\xi\omega_c t_1}\sin(\omega_d t_1 + \phi)}{e^{-\xi\omega_c(t_1+\tau_d)}\sin\left(\omega_d\left(t_1+\tau_d\right)+\phi\right)}$$
$$= \ln e^{\xi\omega_c\tau_d} = \xi\omega_c\tau_d \qquad (2.3\text{-}7)$$

The damped period of motion τ_d is given by

$$\tau_d = \frac{2\pi}{\omega_d} = \frac{2\pi}{\omega_c\sqrt{1-\xi^2}} \qquad (2.3\text{-}8)$$

Hence the log decrement in terms of ξ is given by

$$\delta = \frac{2\pi\xi}{\sqrt{1-\xi^2}} \cong 2\pi\xi \text{ , } For\ \xi < 1 \qquad (2.3\text{-}9)$$

In Fig 2.3-2 the maximum motion on the first cycle of motion is approximately 4.7 mils. The peak to peak motion of the second cycle is 3.5 mils, the third is 2.53 and the fourth is approximately 1.84 mils. The log decrement may be computed from the measured damped responce over several cycles as follows:

$$\delta = \frac{1}{n} ln \frac{Y_1}{Y_n} = \frac{1}{3} ln \frac{4.7}{1.84} = 0.3126$$

Solving for ξ in terms of δ results in the following equation.

$$\xi = \frac{\delta}{2\pi\sqrt{1+\left(\frac{\delta}{2\pi}\right)^2}} = \frac{0.3126}{2\pi \times 1.001} = 0.051 \qquad \textit{(2.3-10)}$$

This is very close to the assumed value and hence the rotor will have an amplification factor of approximately 10 at the unbalance response critical speed.

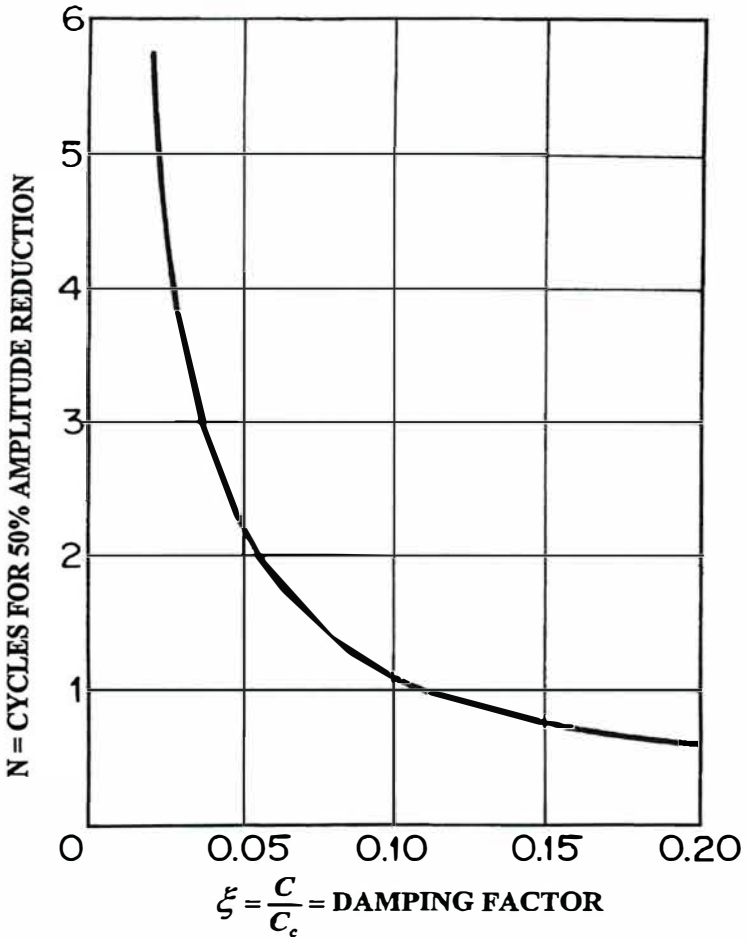

Figure 2.3-3 Number of Cycles N For 50% Amplitude Reduction (*Thomson*)

Fig. 2.3-3 shows that for the case of ξ =0.05, there will be a 50% reduction in amplitude after 2 cycles of motion. This is important for blade loss studies on amplitude attenuation.

In the development of the Jeffcott rotor model, the fixed or pinned supports were generated by assuming a high bearing stiffness. In the first case, bearing stiffnesses of Kb=1.0E8 Lb/In were assumed for each bearing. For this case the ratio of bearing stiffness to shaft stiffness Kb/Ks is over 300. This value of assumed bearing stiffness is excessive and may lead to numerical problems. For example, some finite element codes such as NASTRAN, in their sample model even suggest the use of values as high as 1.0E10 Lb/In support stiffness in order to achieve a pinned support.

Such a large value should never be used in any finite element code as numerical difficulties may arise due to the generation of excessively stiff elements. In practice, bearing or support stiffness values seldom exceed a value of 10.0E6 Lb/In. It is of interest to not that the dynamic stiffness of large fluid film journal bearings often exceed 5-10E6 Lb/In stiffness. In these cases, foundation flexibility must be included in the analysis.

The bearing forces calculated for the high stiffness case of Kb=100.0E6 Lb/In is incorrect for the second bearing due to numerical problems , even for this simple model. A second case was generated in which the bearing stiffness values were reduces to Kb=10.0E6 Lb/In. Fig 2.3-3 represents the transient bearing forces for the No.1 bearing with the bearing stiffness reduced from 1.0e8 to 1.0e7 Lb/In.

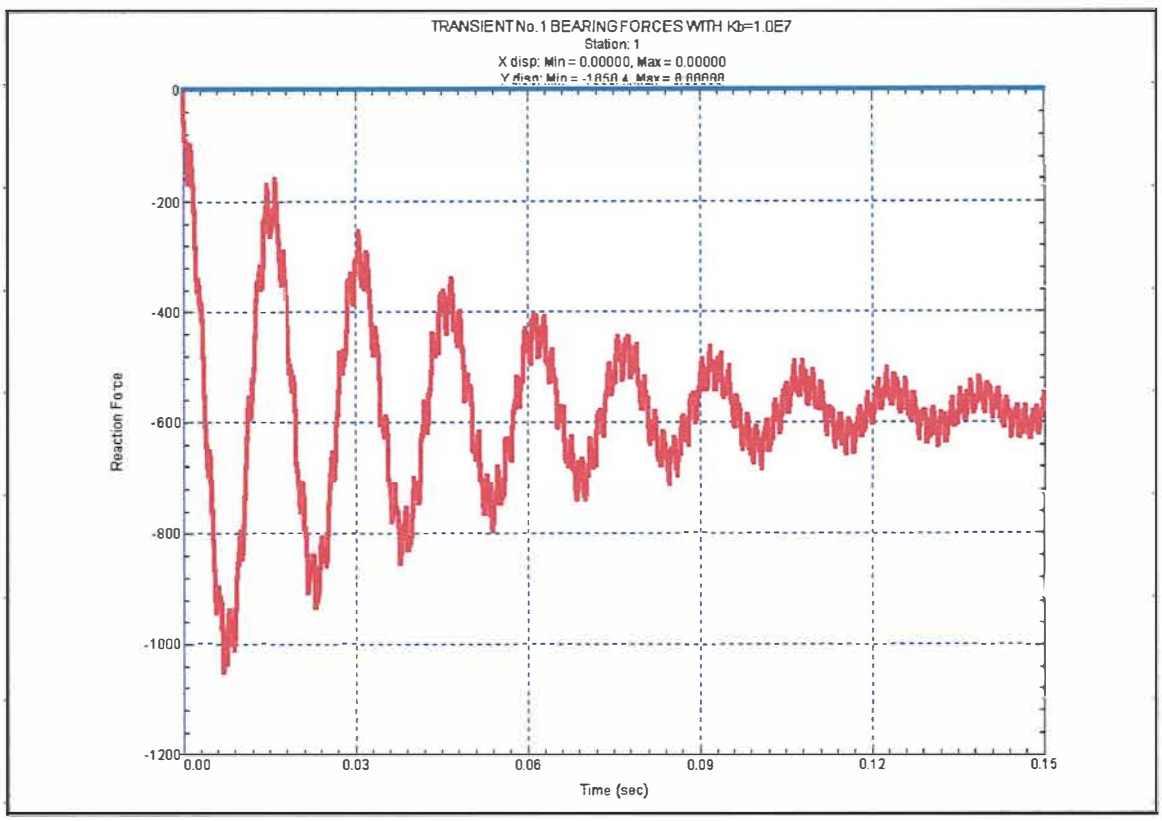

Figure 2.3-4 Transient No. 1 Bearing Forces With Kb=1.0e7 Lb/In

The bearing forces in Fig 2.3-4 for bearing No. 1 are identical to the forces computed for bearing No. 2 and also for the original case with the stiff bearing of Kb=1.0e8. The difference now is that the forces computed for both bearings are identical. The high frequency disturbances are not numerical errors but are due to higher mode excitation

Fig 2.3-4 shows a high frequency oscillation superimposed upon the fundamental Jeffcott 1st critical speed. Normally only 1 mode is associated with the Jeffcott rotor. This would be the case if the shaft is considered as massless and no moment of inertia properties are assigned to the disk.

Since mass has been assigned to the shaft, there are higher modes generated caused by shaft mass. Fig. 2.3-5 represents the Jeffcott 2nd mode. In this mode, the mass center of the disk is a node point and the mode shape appears similar to the uniform beam 2nd mode. Disk gyroscopics, to be discussed later, will further elevate this mode.

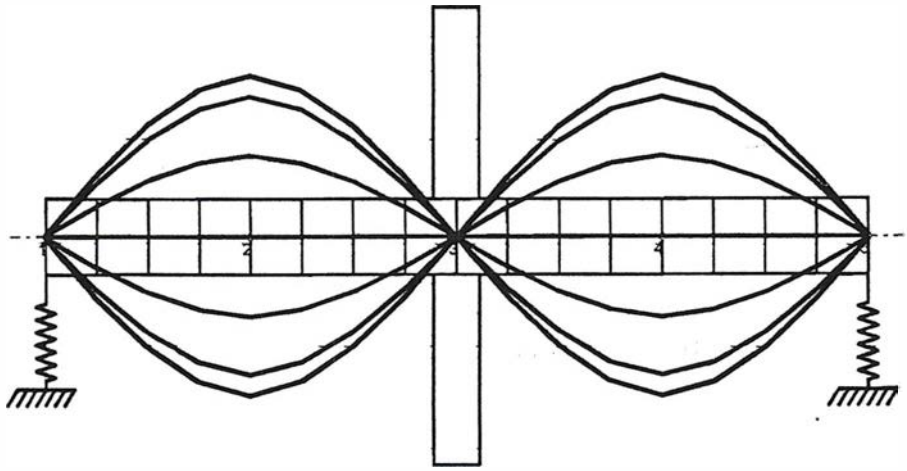

Figure 2.3-5 Jeffcott Rotor 2nd Mode at 23,892 RPM

The transient motion of the rotor due to the gravitational force will not excite this mode. It will also be shown that unbalance at the disk also will not excite the second mode. Fig. 2.3-6 represents the 3rd mode for the Jeffcott rotor.

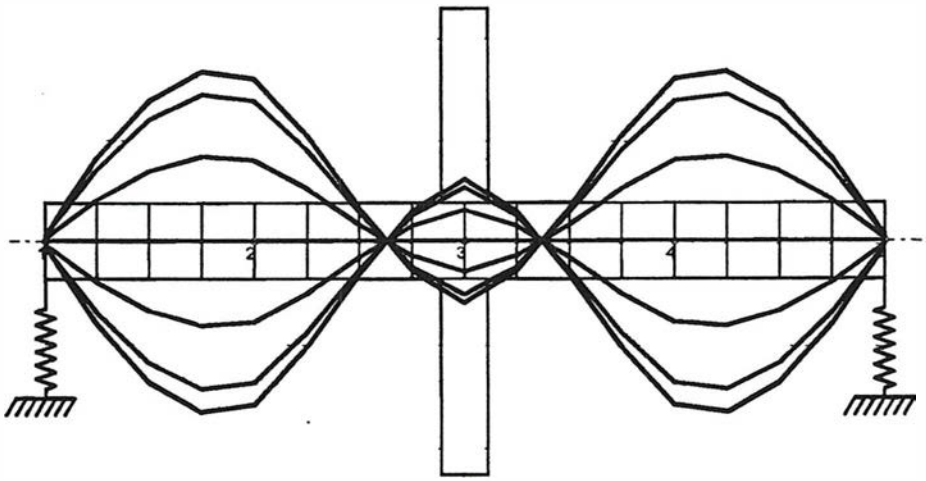

Figure 2.3-6 Jeffcott Rotor 3rd Mode At 41,117 RPM

The 3rd mode may be excited by the initial transient motion of the system. Thus increasing the number of time steps in the analysis will not smooth out the bearing transient response.

2.4 Unbalance Response of Jeffcott Rotor

The unbalance response of the Jeffcott rotor will be evaluated with a radial unbalance at the central disk. The amount of unbalance will be equal to the Jeffcott modal mass offset by 1 mil. The rotor unbalance eccentricity may be represented as follows:

$$U_u = M_{modal} e_u = m_u R \qquad \textbf{Where} \quad m_u / M_{modal} << 1 \tag{2.4-1}$$

The unbalance of the rotor U_u may be considered as the displacement of the effective rotor mass a small distance or eccentricity from the axis of rotation. This same effect could be seen as equivalent to a small weight placed at a distance R radially on the disk. The theory of rotor dynamics and balancing assumes that the unbalance weights are small in comparison to the total rotor weight, or in this case the rotor modal mass or weight.

The units of unbalance will depend upon whether one uses consistent finite element units (option 0) or English engineering units (option 2) as shown in Fig. 2.4-1. The specification of consistent units would be as follows:

$$U_u = \frac{800\,Lb}{396\,In/Sec^2} \times 0.001\,In = 0.002\;Lb - Sec^2$$

In English engineering units, ***DYROBES*** uses oz-in for units of unbalance.

$$U_u = 800\,Lb \times 0.001\,In \times 16\,oz/Lb = 12.8\,oz - In$$

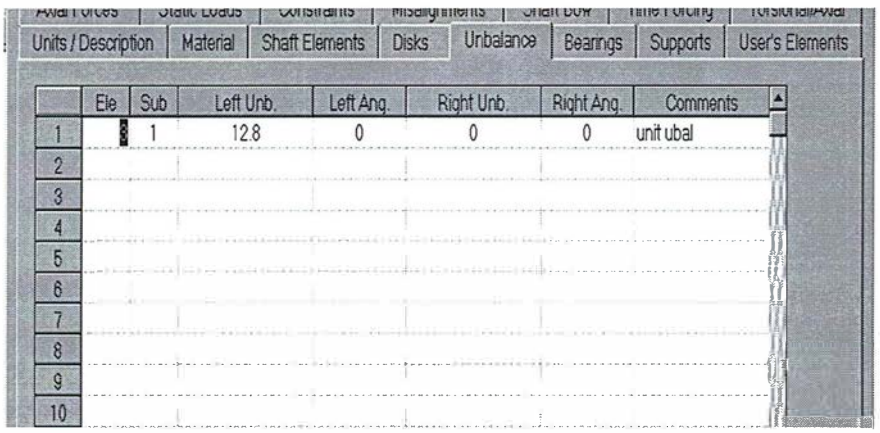

Figure 2.4-1 Specification of Unbalance Using Option 2-Oz-In

The rotating force generated by the unbalance is given by:

$$F_u = Me_u\omega^2 = U_u\omega^2\,,\,Lbs$$

$$For\;N = 3{,}900\,RPM\,,F_u = 0.002 \times \left(\frac{3900 \times 2\pi}{60}\right)^2 = 333.5\,Lb \tag{2.4-2}$$

At this speed, (the critical speed), the bearing reaction for a rigid rotor would be 167 Lb. It will be seen that the actual bearing forces will be over 10 times this value as predicted by rigid rotor theory.

Disk Unbalance Response

Figure 2.4-2 represents the amplitude of motion(0-peak) at the rotor center, station 3.

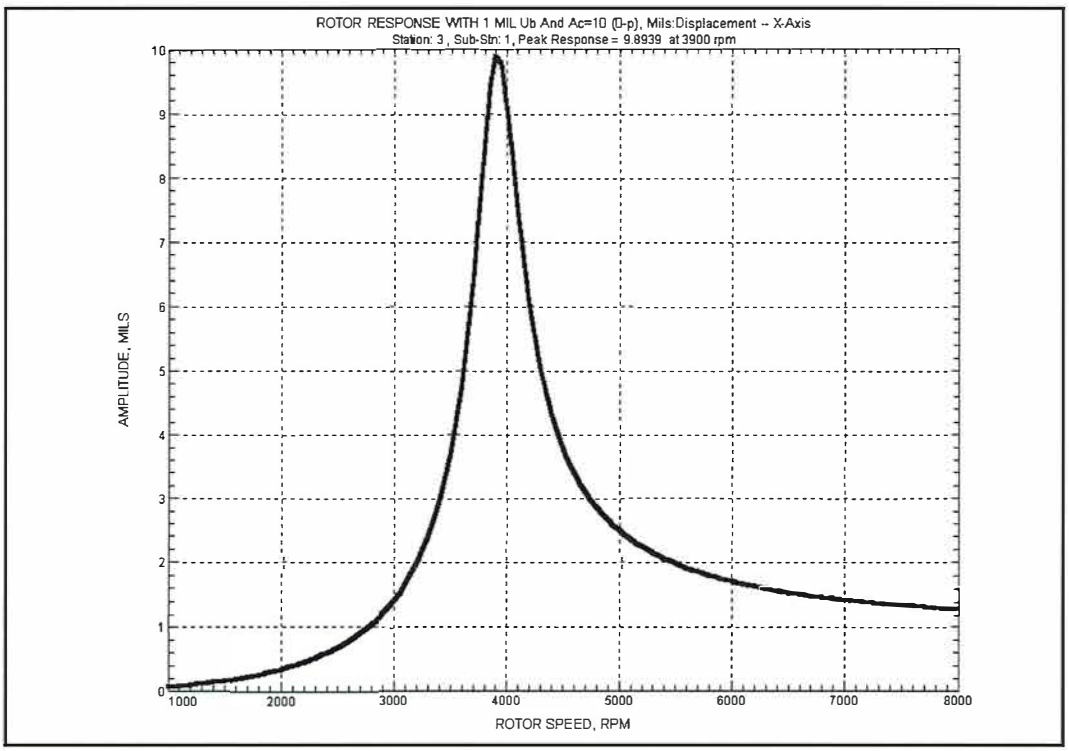

Figure 2.4-2 Jeffcott Rotor Synchronous Unbalance Response With 1 Mil Modal Unbalance Eccentricity - Ac = 10 , (0-P) Mils Amplitude

In Fig. 2.4-2, the amplitude is in 0-peak motion. Since the damping was selected to generate an amplification factor of 10, we see that the peak amplitude at the critical speed of 3,900 rpm is approximately 10 mils radial displacement. As the speed increases well above the first critical speed, the radial amplitude of motion will approach 1 mil, which represents the disk unbalance eccentricity. The rotor mass center has inverted and is rotating about the spin axis.

Amplification Factor

The rotor amplification factor may be estimated by several means from the plot of the rotor synchronous response vs speed. The basic definition of the amplification factor is the ratio of

$$A_c = \frac{X_{critical\ speed}}{X_{N\to\infty}} = \frac{X_{cr}}{e_u} = \frac{10_{mils}}{1_{mil}} = 10 \qquad \textbf{(2.4-3)}$$

This method is not always practical, since the rotor amplitude is not measured to a high enough speed. Also, with most multistage compressors and turbines, the effects of the second critical speed will begin to appear. Another more practical method is the half power point method derived from electrical engineering. This method is based upon the assumption of a constant forcing function, but it represents a good approximation of the amplification factor for light to moderate damping. If damping is heavy, then amplification factor at the critical speed is obviously not a problem.

Half Power Point Method

A good approximation of the rotor amplification factor for a response critical speed is by the application of the half power point method. In this method, a horizontal line is constructed equal to 0.707 of Xmax at the critical speed. The amplification factor is given by dividing the critical speed by the band width as determined by the .707 Xmax line.

$$A_c = \frac{N_c}{\Delta N_{.707}} \qquad \textbf{(2.4-4)}$$

Fig. 2.4-3 represents the unbalance response for the restricted speed range of 3,000 RPM to 5,000 RPM in order to compute the speed increment at the half power points.

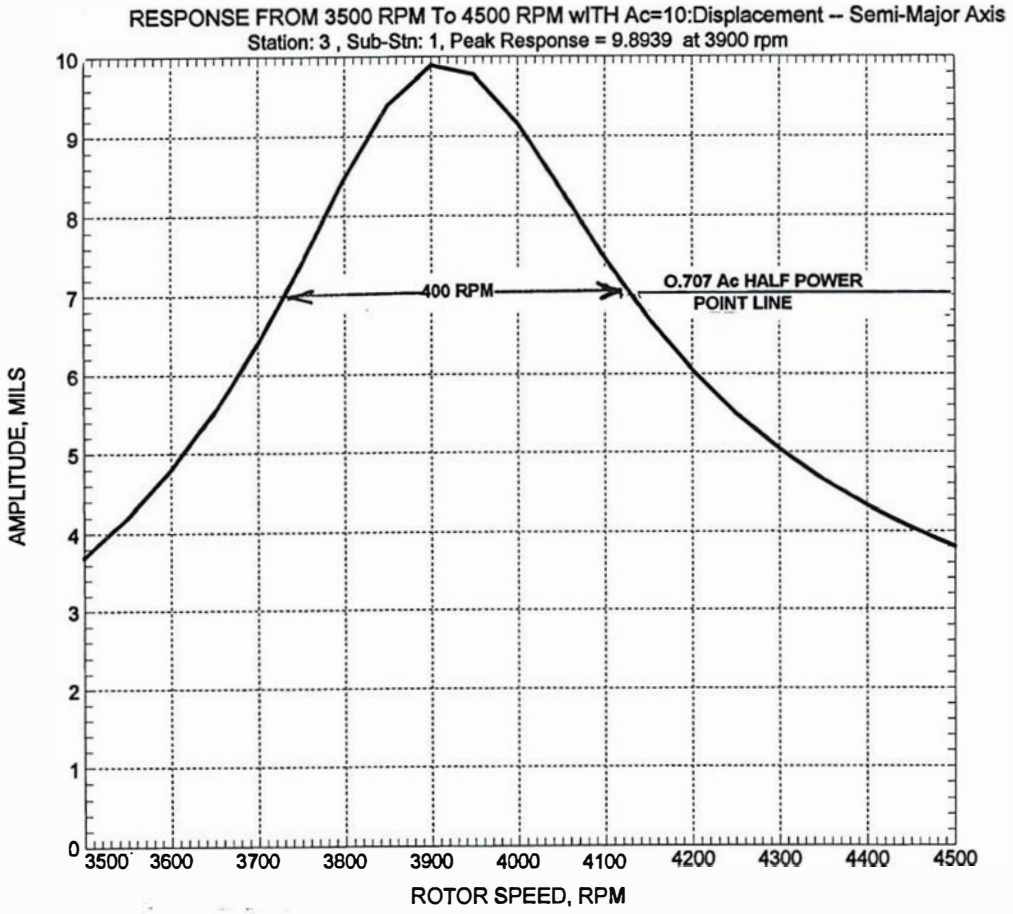

Figure 2.4-3 Jeffcott Rotor Response From 3,000 RPM to 5,000 RPM

The half power point line would be at the amplitude line of 7 mils. The frequency increment at this line is ΔN=400 RPM. The amplification factor Ac is thus 3,900 /400=9.75.

The half power point method is a reasonable procedure to estimate the rotor unbalance response based upon experimental data. It should be noted that the amplification factor predicted will vary somewhat depending upon the position along the shaft. For example, the amplification factor predicted near a bearing will usually result in a lower value then that predicted near the center span.

With multi mass rotors, it is not practical to compute the amplification factor based upon the ratio of the amplitude at the critical speed and the unbalance eccentricity. The half power point method provides a practical procedure to compute, not only the first, but also higher amplification factors.

Bode Plot

The bode plot for the Jeffcott rotor shows both the amplitude of motion and the phase angle change. The amplification factor may also be determined from the rate of change of the phase angle while passing through the critical speed region. The faster the rate of change in phase while passing through the critical speed region, the higher the amplification factor. Therefore, with high amplification factor rotors, it is not desirable to attempt to balance near the critical speed region using the influence coefficient method due to the rapid rate of change of phase with only small changes in speed.

Fig. 2.4-4 represents the amplitude and phase plot for the rotor mass center. The combination of the two plots together is referred to as the Bode plot. It is seen that at the critical speed, the phase angle is 90^0. The shaft deflection vector is lagging the unbalance forcing function by 90^0 at the critical speed. If the shaft should rub while passing through the critical speed, this rub mark would indicate the ***high spot*** . A balance correction weight then should be placed at 90^0 from the rub mark opposite the direction of rotation. This would then place a correction weight at 180^0 from the shaft ***heavy spot***.

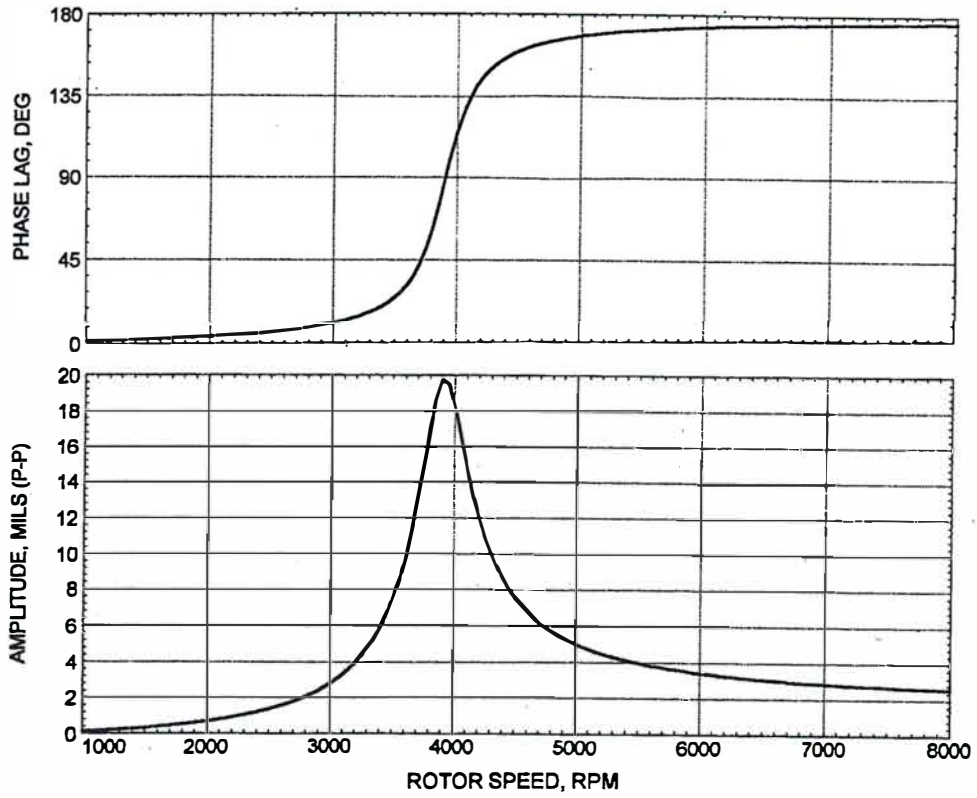

Figure 2.4-4 Bode Plot For Jeffcott Rotor Showing Amplitude And Phase

The rotor amplitude of motion is given by:

$$A(\omega)_{0-p} = \frac{Me\omega^2}{\sqrt{\left(K - M\omega^2\right) + \left(C\omega\right)^2}} \qquad (2.4\text{-}5)$$

Phase Angle For Various Values Of ξ

The rotor damping ratio ξ will determine the rate of change of the rotor phase angle while passing through the critical speed region. Fig. 2.4-5 represents the phase angle plots vs the dim. speed ratio f. The value of $f = 1$ represents the dimensionless critical speed. At this value, all of the damping curves pass through the same point at the phase angle of 90^0.

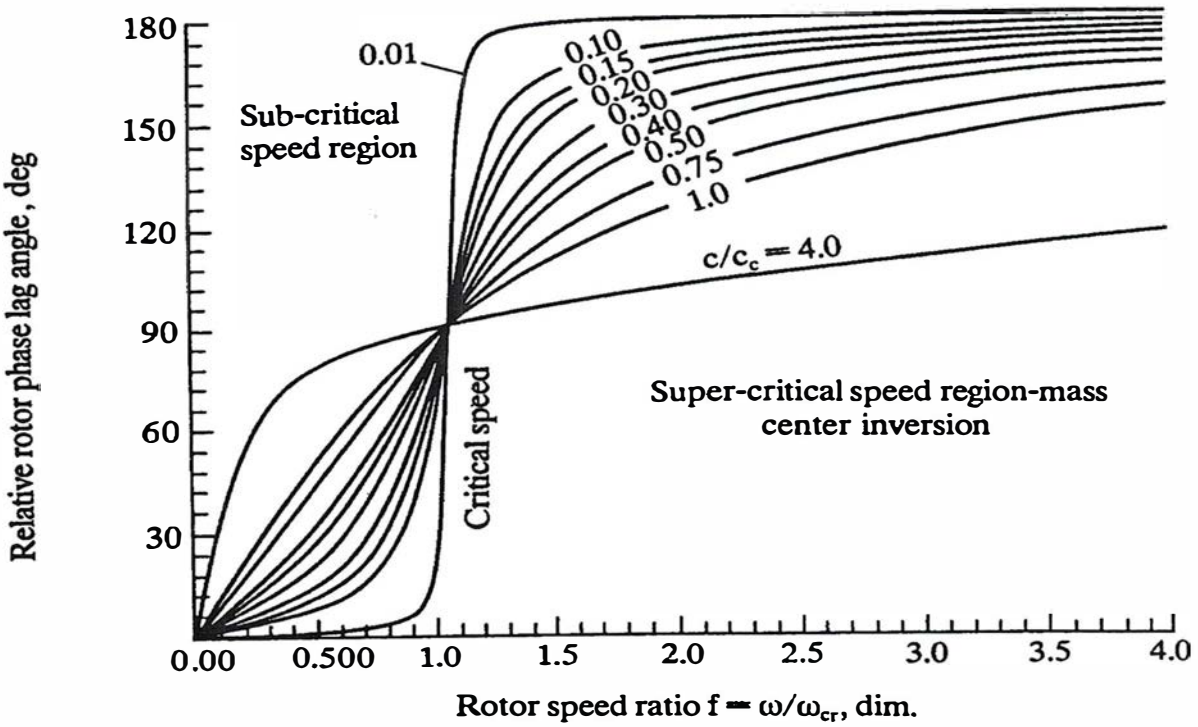

Figure 2.4-5 Rotor Phase Angle Vs Dimensionless Frequency Ratio For Various Values Of ξ

The relative phase angle change between the displacement vector and the unbalance forcing function is given by:

$$\phi = tan^{-1}\left(\frac{C\omega}{K - M\omega^2}\right)$$

In dimensionless form **(2.4-6)**

$$\phi = tan^{-1}\left(\frac{2\xi f}{1 - f^2}\right)$$

As the speed greatly exceeds the critical speed, $f >> 1$, then the phase angle approaches 180. This implies that the rotor has self balanced and is rotating about the mass center with a radial orbit of e_u. It is also important to note that if ξ exceeds 0.5, then there is no peak critical unbalance response speed observed. This corresponds approximately to a log dec value of $\delta = \pi$.

Lightly damped rotors are difficult to balance within ±10% of the critical speed by means of the influence method of balancing. The three trial weight method is preferred.

Polar Plots

The rotor amplitude and phase may be combined to produce a polar diagram. The polar diagram is useful in the determination of the rotor unbalance location and also to indicate possible initial bowing of the shaft.

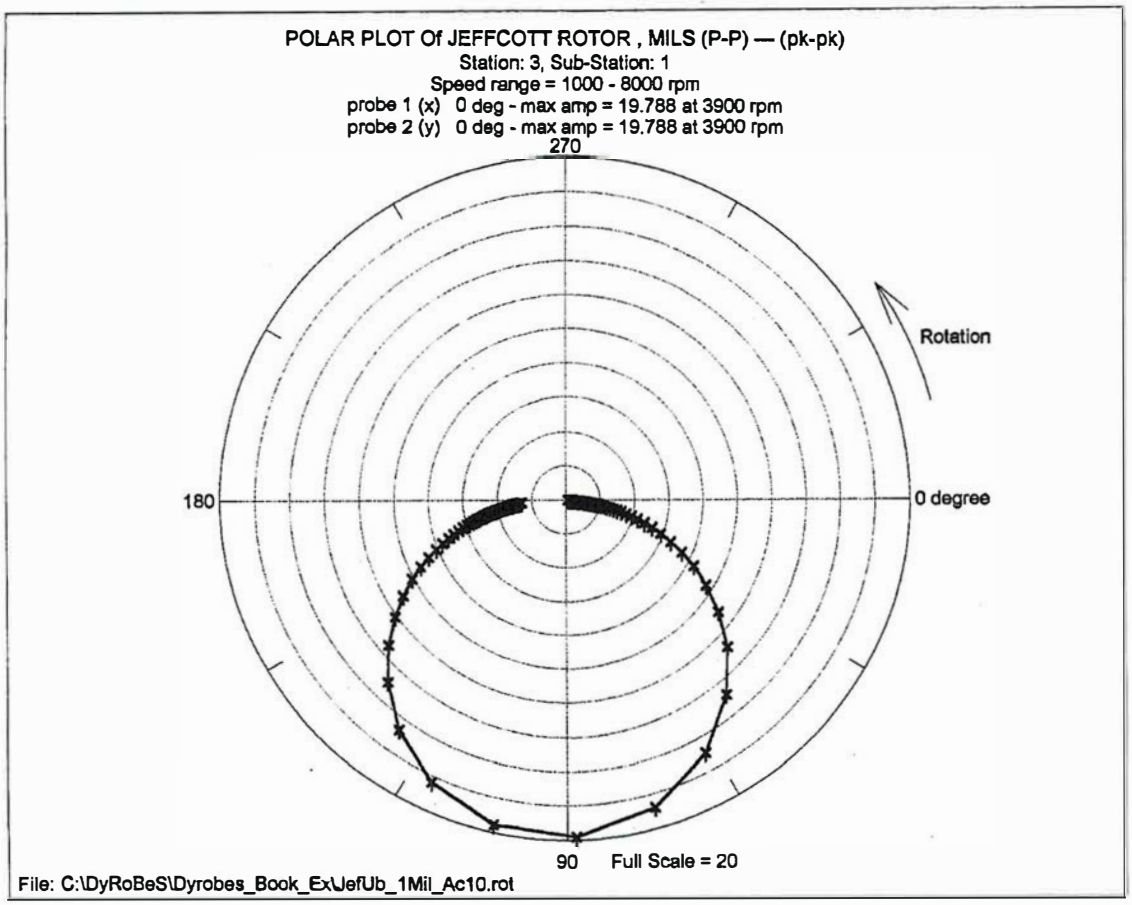

Figure 2.4-6 Polar Plot Of Rotor Motion With Radial Unbalance Of e_u = 1Mil At 0 Deg

At low speed, the polar plot starts off tangent to the 0 Deg axis. This is because the unbalance is in phase with the deflected shaft at low speeds, below the critical speed. As the speed increases, the deflection phase angle begins to lag the forcing function. Therefore, the phase angle increases opposite to the direction of rotation. At the critical speed, the phase angle is 90^0. The marks on the polar plot are for equal time increments. Notice that at the critical speed, the phase is changing the most rapid.

As the speed continues to increase, the phase angle approaches 180^0. The amplitude of motion becomes smaller and approaches $2x\boldsymbol{e}_u$, the unbalance eccentricity. For balancing, an initial trial weight should be placed at the 180^0 position with a magnitude of $\mathbf{U}_b = \mathbf{M}_{modal} x \mathbf{e}_u$. If a line is constructed to the maximum deflection vector (at 90^0), then a perpendicular vector is drawn from this line opposite the direction of rotation. This gives a good approximation for the location of a rotor initial trial weight ***Ut*** for balancing.

Rotor Displacement And Mass Center Relationships At Various Speeds

Fig. 2.4-7 represents the shaft orbit recorded at the rotor critical speed of 3,900 RPM. At this exact speed, the phase of the rotor motion is lagging the unbalance forcing function by 90^0.

The radius of the rotor amplitude at the critical speed is 9.89 mils. Since the rotor unbalance eccentricity is approximately 1 mil, then the amplification factor at the critical speed is approximately 10. The amplitude recorded on a Bently proximeter probe on peak to peak would be recorded as 19.7 mils.

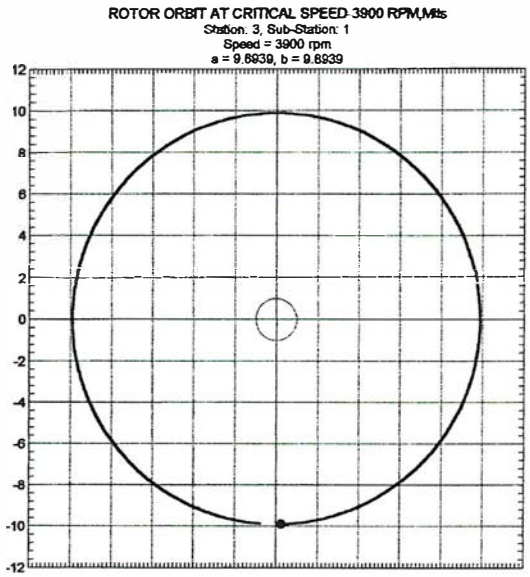

Figure 2.4-7 Rotor Orbit At Critical Speed - N = 3,900 RPM

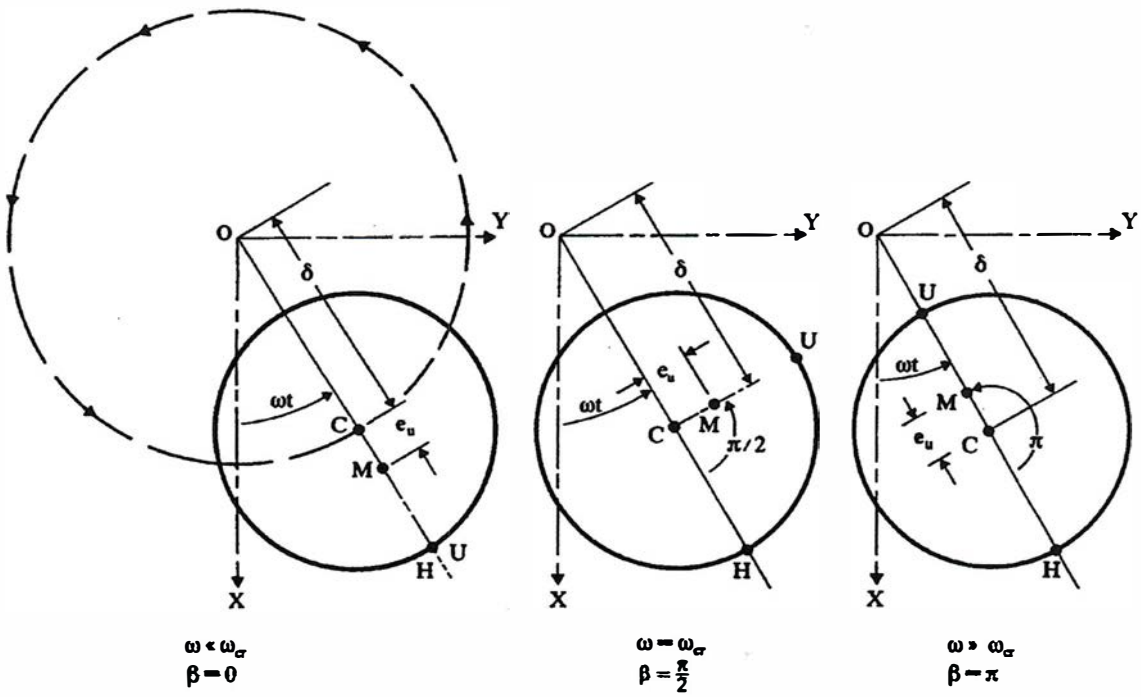

Figure 2.4-8 Rotor Amplitude-Phase Behavior Below, At And Above The Rotor Critical Speed

In the orbits shown, the rotor whirl motion is counter clockwise. The Bently probe convention is to show a blank space and then an indicator mark. This mark is generated by a keyphaser probe. In this case the keyphaser is in the x dir. Fig. 2.4-8 shows the rotor response at various speeds with respect to the critical speed. At low speeds when $\omega << \omega_{cr}$, then the mass center vector $\vec{CM}$ is in line with the shaft deflection vector $\vec{OC}$. The point labeled **H** represents the shaft ***HIGH*** spot and **U** is the unbalance or ***HEAVY*** spot.

Phase At Critical Speed

The center diagram shows the rotor deflection vector $\vec{OC}$ at the critical speed when $\omega = \omega_{cr}$. At this speed the deflection vector is lagging the unbalance vector $\vec{CM}$ by 90^0. The line of $\vec{OC}$ extended represents the high spot **H** on the shaft. At this speed it is seen that the high spot **H** on the shaft is 90^0 lagging the heavy spot **U** on the rotor. If, for example, a seal rub occurred on the shaft while passing through the critical speed, it would make a mark at the point **H** on the shaft. The proper location to place a trial balancing weight then would be at a spot lagging the rub mark by approximately 90^0. It would be improper to place the trial weight 180^0 out of phase to the rub mark as this would add to the total unbalance in the rotor.

Phase Above Critical Speed

As the rotor speed exceeds the rotor critical speed, the phase angle increases from 90^0 to 180^0 at the speed increases well above the critical speed. At very high speeds of rotation, there is no further increase as the rotor system has now ***self balanced***. By self balancing, we mean that the rotor mass center lies along the shaft spin axis. No further increase in amplitude will occur until a higher order mode is encountered due to shaft mass effects. From the polar plot of Fig. 2.4-6 it is seen that the p-p orbit approaches 2 mils at 180^0. This point indicates the location for the rotor trial weight placement for balancing.

Bently Probe Phase Convention

Fig. 2.4-9 shows the typical Bently prox probe phase lag convention. When the keyphaser

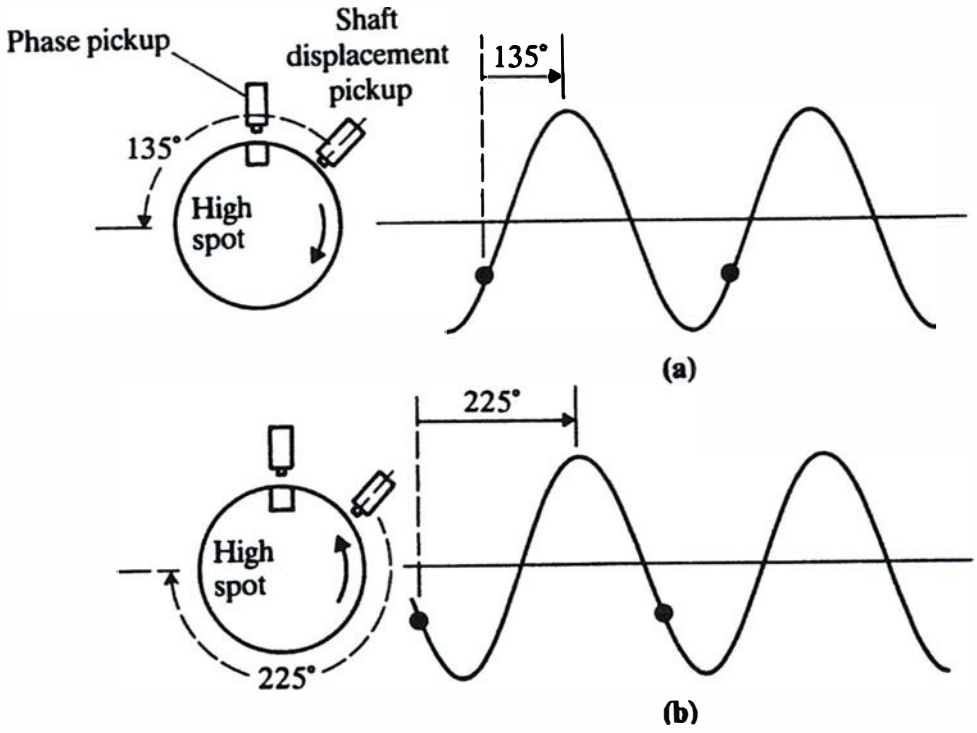

Figure 2.4-9 Bently Probe Lag Phase Convention For Clockwise And Counter Clockwise Rotation

probe lines up with the shaft notch, the zero reference is set. The high spot is measured from the probe opposite the direction of rotation. This applies to both ***CC*** and ***CCW*** rotation.

Jeffcott Rotor With Arbitrary Unbalance

Fig. 2.4-10 represents the Jeffcott rotor with an arbitrary placement of the unbalance weight on it. The mass center location is measured from the keyphaser opposite the direction of rotation. The angle of the mass center measured from the keyphaser is Φ_m.

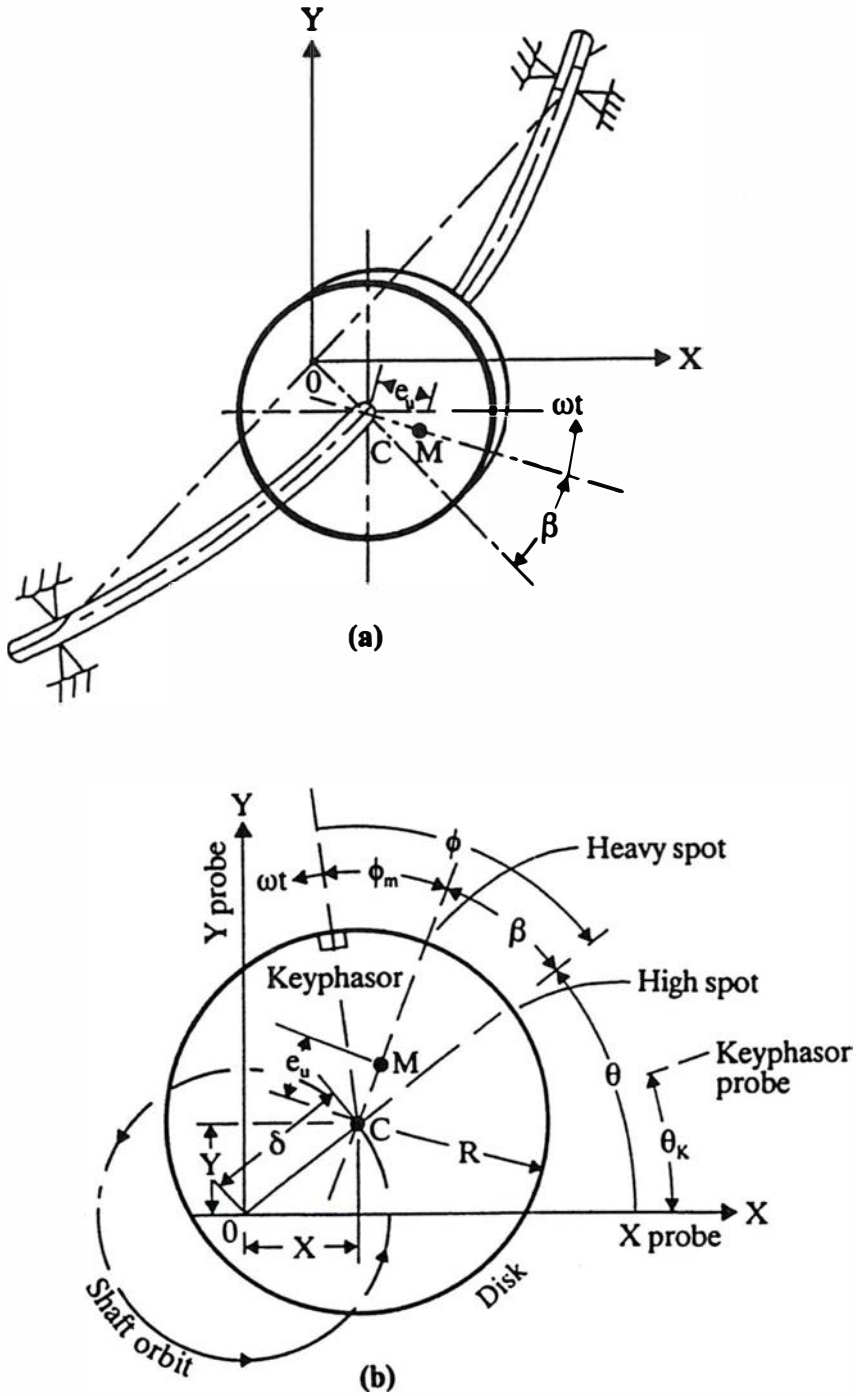

Figure 2.4-10 Jeffcott Rotor Showing Arbitrary Unbalance Location

The relative phase angle measured from the mass center to the deflection vector is β. The absolute phase angle as measured from the keyphaser to the heavy spot is $\Phi = \Phi_m + \beta$. It is apparent from Fig. 2.4-10 that the high spot does not correspond to the rotor heavy spot.

Bearing Forces Transmitted

Fig. 2.4-11 represents the bearing forces transmitted for the flexible Jeffcott rotor in comparison to the bearing forces transmitted as if the rotor were perfectly rigid. The computation of rigid bearing forces may be accomplished by ***DYROBES*** by assuming a high modulus of elasticity of E=30.0e8. This places the first critical speed well above the operating speed and creates a rigid rotor. In Fig. 2.4-11 the maximum bearing forces transmitted occurs at the first critical speed at 3900 RPM with a magnitude of 1935 Lb. The rigid bearing forces transmitted at the critical speed to each bearing is given by:

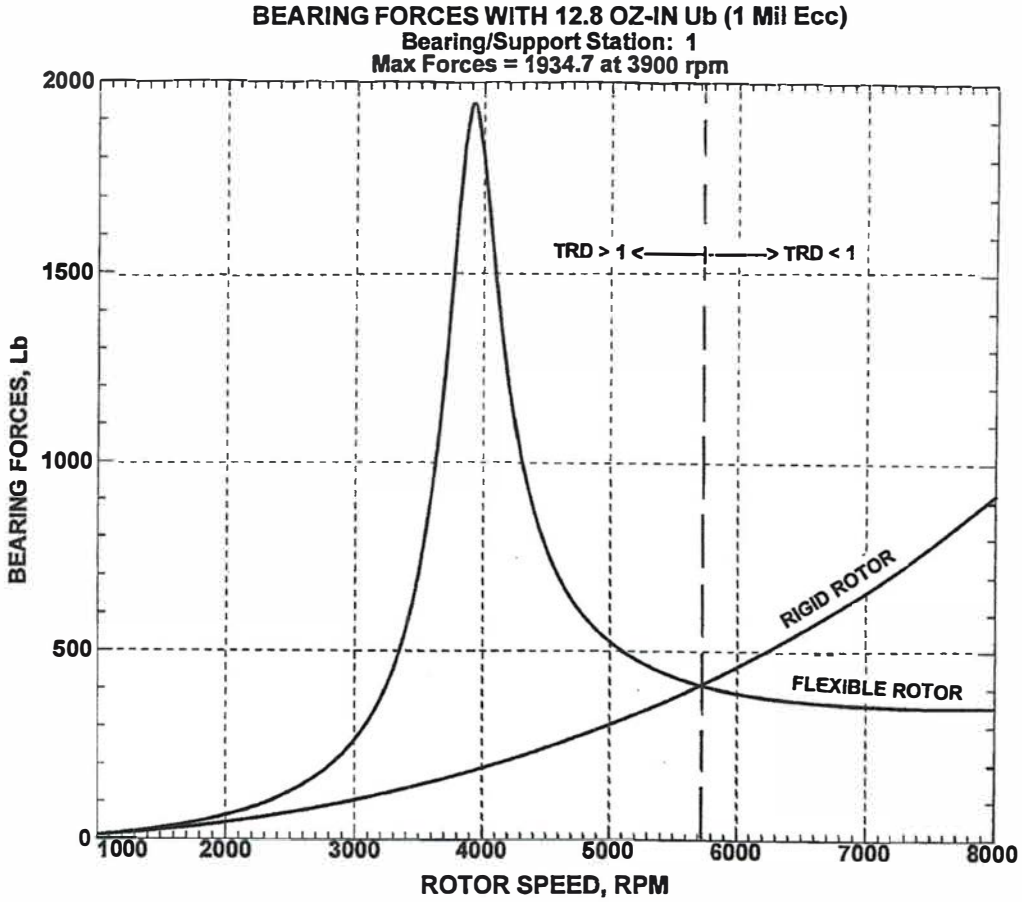

Figure 2.4-11 Bearing Forces Transmitted For Flexible And Rigid Rotor

$$F_{brg} = \frac{Me_u}{2}\omega^2 = \frac{12.8\,oz\text{–}in}{2\times 16\,oz/lb\times 386.4}\left(\frac{3900\times 2\pi}{60}\right)^2 = 173\,Lb \qquad (2.4\text{-}7)$$

By dividing the maximum bearing force at the critical speed by the theoretical forces generated by a perfectly rigid rotor, one may compute the rotor dynamic transmissibility at the critical speed. This value is similar to the rotor amplification factor and may be even higher. The value of **TRD** at the critical speed is equal to 1,935 Lb/173 Lb=**11.8**.

It is important to note that at speeds below $N < \sqrt{2}N_{cr}$, the dynamic transmissibility function is greater than 1. At speeds above 1.4Ncr, the **TRD** values become less than 1.

Dynamic Bearing Transmissibility

The dynamic bearing Transmissibility may be defined as the ratio of the bearing forces transmitted at any speed to the bearing forces transmitted assuming that the rotor is perfectly rigid. The ***TRD*** ratio is given by the following equation.

$$TRD(\omega) = \frac{F_{bearing-flexible\ rotor}}{F_{bearing-rigid\ rotor}} \qquad (2.4\text{-}8)$$

For the case of the Jeffcott rotor on pinned supports, the bearing transmitted force ratio may be computed as follows:

$$TRD(\omega) = \frac{K\,A(\omega)}{Me_u\omega^2} = \frac{K}{\sqrt{\left(K - M\omega^2\right)^2 + \left(C\omega\right)^2}} = \frac{1}{\sqrt{\left(1-f^2\right)^2 + \left(2\xi f\right)^2}} \qquad (2.4\text{-}9)$$

For the dimensionless speed value f at which the ***TRD*** value is unity, we have

$$TRD(\omega^*) = 1 = \frac{1}{\sqrt{\left(1-f^{*2}\right)^2 + \left(2\xi f^*\right)^2}} \approx \frac{1}{\sqrt{\left(1-f^{*2}\right)^2}}\ \textit{For low damping} \qquad (2.4\text{-}10)$$

Solving for f^* for the cross over speed we obtain:

$$1 = \frac{1}{\left|\left(1-f^{*2}\right)\right|} = \frac{1}{f^{*2}-1}\ since\ f^* > 1$$

$$\therefore f^{*2} = 2\ \textit{or}\ f^* = \sqrt{2}\quad ;\quad N^* = 1.414\,N_{cr} \qquad (2.4\text{-}11)$$

From Eq. ***2.4-11*** we see that the dynamic transmissibility function is not reduced below 1 until the rotor has exceeded 40% above the critical speed. This is an important design factor with large utility fans. It has been the design practice to attempt to design fans as rigid rotors operating below the first critical speed.

This has lead to the design of stiff fans on rolling element bearings operating below the first critical speed. The results of such a design practice has been the development of fans that are difficult to balance and with very short bearing life. The results of such design practices has caused utilities millions of dollars in repairs and loss of power generation due to excessive down times. Proper fan design would place the first critical speed at least 40% below the running speed. In order to accomplish this with rolling element bearings, a flexible damper support would need to be incorporated into the design in order to avoid problems passing through the first critical speed region and also to avoid stability problems.

Unbalance At Arbitrary Location

The rotor unbalance may be specified as acting at an arbitrary location. **Fig. 2.4-10**, for example, shows the arbitrary unbalance located at an angle of Φ_m drawn counter to the direction of rotation. This places the unbalance weights and phase angular measurements both in a phase lag convention. In order to use the phase lag convention, **Fig 2.4-12** shows the specification of the unbalance weight of 12.8 oz-in at element 3 at the lag angle of 45^0.

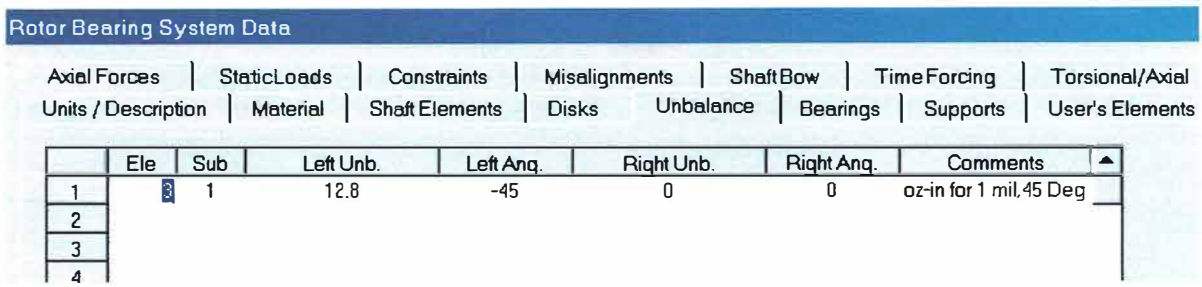

Figure 2.4-12 Specification Of 12.8 Oz-In Unbalance At 45 Deg Lag Angle (e_u =1 Mil)

Balancing computations and measurements using noncontact prox probes usually employ the lag phase convention. **Fig. 2.4-13** represents the polar plot for the Jeffcott rotor with the unbalance shifted 45^0 against rotation from the keyphasor position.

In **Fig. 2.4-13**, a line is drawn to the maximum amplitude of 19.82 mils p-p at the critical speed of 3925 RPM. This value is slightly larger than the value shown in **Fig. 2.4-6** since a finer speed increment of 25 RPM was used in the calculations. The maximum amplitude vector is drawn at the phase angle of $\Phi_{cr} = 135^0$.

The maximum amplitude vector lags the plane of unbalance by 90^0 .

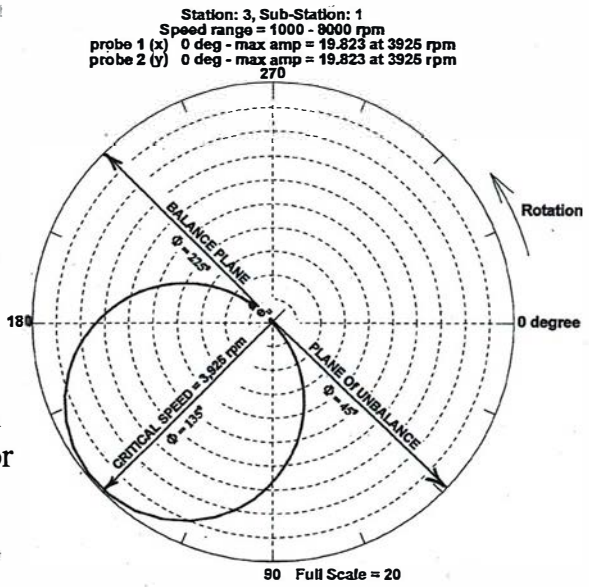

Fig. 2.4-13 Polar Plot With 45^0 Phase Lag

It should be noted that the amplitude vector at low speed is tangent to the plane of unbalance at 45^0. As the speed increases, the lag angle and amplitude of synchronous motion increase until a maximum value is reached at the critical speed. As the speed is increased further, the amplitude reduces and the phase angle continues to increase to a maximum theoretical value of 180^0. In an actual rotor, one may encounter phase angle increases above 180^0. This is an indication that a higher order critical speed is being entered into.

In the limit, the amplitude in the polar diagram will reduce to $2xe_u$, twice the unbalance eccentricity (since this plot is in peak to peak motion).

A tangent vector drawn from the origin and passing through the projected location of point $2e_u$ defines the balance plane. The balance correction should be placed at this location. A trial magnitude may be estimated from the product of the modal mass Mxe_u.

2.5 Response of Jeffcott Rotor With Shaft Bow

Rotor Description

The generalized Jeffcott rotor with shaft bow and unbalance is shown in Fig. 2.1. The rotor has an initial shaft bow of δ_r. At low speeds, the center of the disk, point C moves in a circular orbit of radius δ_r about the origin. The shaft bow may be caused by improper attachment of the disk to the shaft, gravitational sag or it may be thermally induced. If the shaft bow is excessive, then high bearing forces will be encountered and the rotor may be difficult to balance. It will be seen that the forced synchronous response due to shaft bow will appear very similar to the characteristics of forced response due to radial disk unbalance.

Equations of Motion With Shaft Bow

The equations of motion with shaft bow are similar to Eq. *(2.2-4)* as follows:

$$\begin{aligned} M\ddot{X} + C_s\dot{X} + K_s\left(X - X_r\right) &= Me_u\omega^2 \cos\left(\omega t - \phi_m\right) \\ M\ddot{Y} + C_s\dot{Y} + K_s\left(Y - Y_r\right) &= Me_u\omega^2 \sin\left(\omega t - \phi_m\right) \end{aligned} \qquad (2.5\text{-}1)$$

The shaft bow in complex notation may be expressed as:

$$\delta_r = X_r + iY_r = \vec{Z}_r \qquad (2.5\text{-}2)$$

The total synchronous motion due to the combination of both unbalance and shaft bow is:

$$\vec{Z} = Z_u + Z_r = \frac{e_u f^2 e^{-i\phi_m} + \delta_r e^{-i\phi_r}}{1 - f^2 + i2\xi f} \qquad (2.5\text{-}3)$$

The total motion of the shaft is a vector combination of unbalance and shaft bow. Note that both components share the same common denominator. Thus both effects have similar amplification factors. Hence it is possible to balance out shaft bow with suitable unbalance.

Specification of Shaft Bow

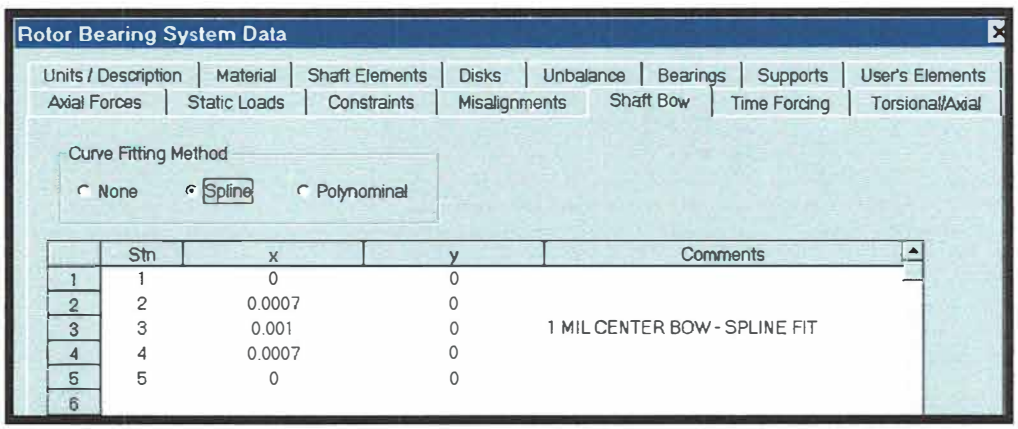

Figure 2.5-1 Specification of 1 Mil Shaft Bow At 0 Deg

Fig. 2.5-1 represents the specification of the 1 mil shaft bow at the 0 deg location. If one chooses a cubic spline curve fit, it is only necessary to pick the amplitude at the disk and set the bow vector to 0 at the bearings. The x-y coordinate system is a relative coordinate system attached to the shaft. The x axis may be assumed to pass through the keyphasor mark and the y axis forms a right handed reference system and is positive in the direction of rotation.

Response With Bowed Rotor

Fig. 2.5-2 represents the response of the Jeffcott rotor with a 1 mil bow at the zero deg location. The amplitude , shown as 0-P starts at 1 mil at low speed. This initial amplitude represents the bow in the shaft. It should be noted, that if a prox probe is placed on the disk, then an initial mechanical vector may also be observed which is not shaft bow. This vector is simply the mechanical runout of the disk and does not contribute to the rotor excitation.

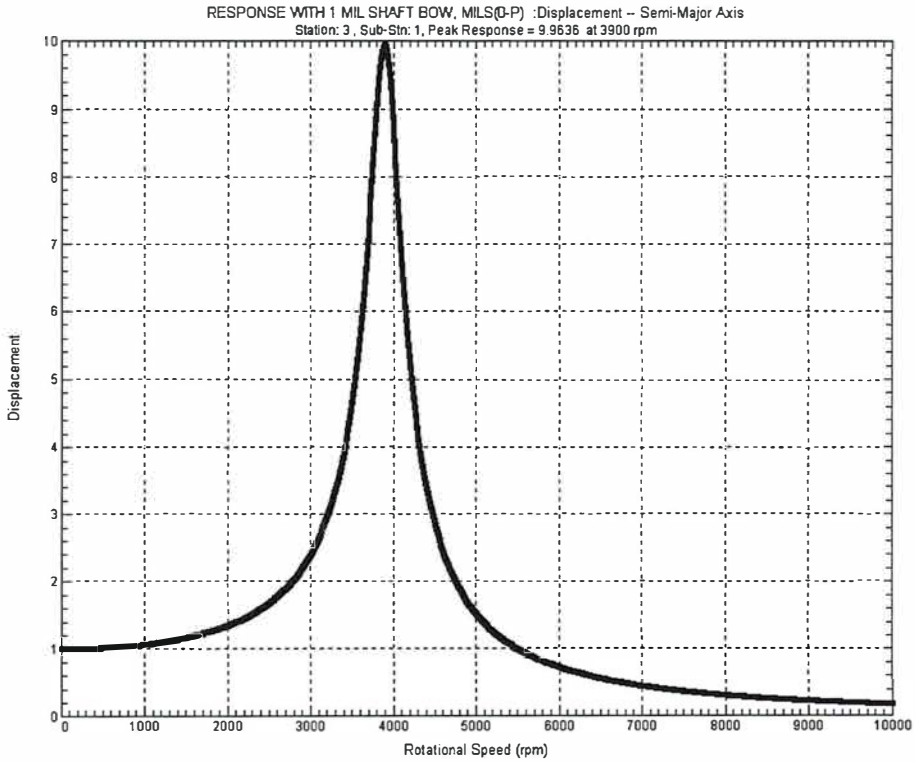

Figure 2.5-2 Jeffcott Rotor Response With 1 Mil Shaft Bow

In Fig. 2.5-2, it is seen that the rotor motion is initially 1 mil. At the critical speed, the maximum response is approximately 10 mils since the amplification factor is 10. From Eq. ***2.5-3***, it is seen that the amplification factor at f=1 for both unbalance and bow is:

$$A_{cr}\big|_{f=1} = \frac{1}{i2\xi} \qquad \textit{(2.5-4)}$$

Therefore it is seen that the bow vector δr has the same effect as the unbalance eccentricity vector e_u at the critical speed. It is also apparent that the balancing requirement for the Jeffcott rotor with shaft bow is similar to the balancing requirement with the radial displacement of the rotor modal mass center.

$$U_b = w_{balance} R_{disk} = \delta_r W_{modal} = e_u W_{modal} \qquad \textit{(2.5-5)}$$

Thus a small amount of shaft bow may require a very large balance correction weight to compensate for it. In the above example with the 1 mil bow, 12.8 oz-in would be required to balance out the shaft bow. With large turbines or compressors, it is not usually practical to balance out large initial shaft bow vectors. It is also apparent that initial thermal bows may lead to high rotor vibrations.

Fig. 2.5-3 represents the peak-to-peak polar plot with 1 mil shaft bow. The vibration at low speed is shown as 2 mils. The polar plot with shaft bow is circular in nature. At high speeds, well above the critical speed, the bow straightens out and the amplitude goes to zero.

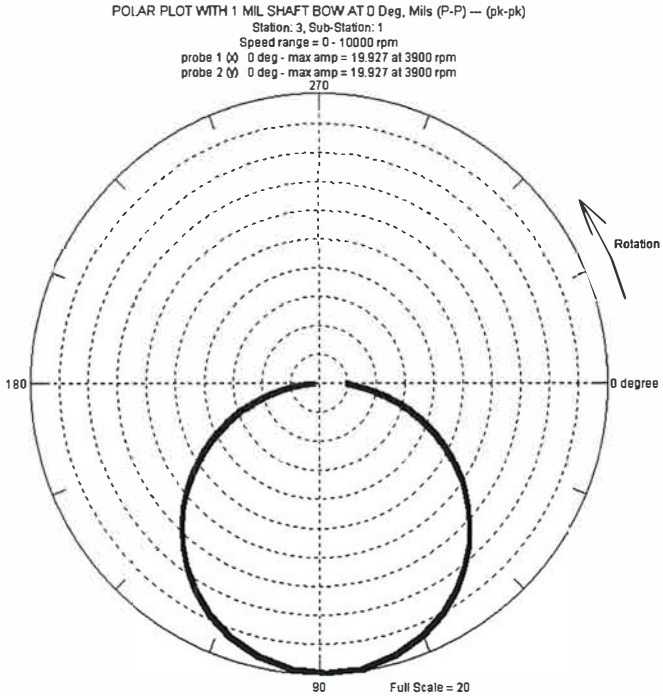

Figure 2.5-3 Polar Plot Of Jeffcott Rotor With 1 Mil Bow

Bearing Forces With 1 Mil Bow

Fig. 2.5-4 represents the bearing forces transmitted with 1 mil shaft bow.

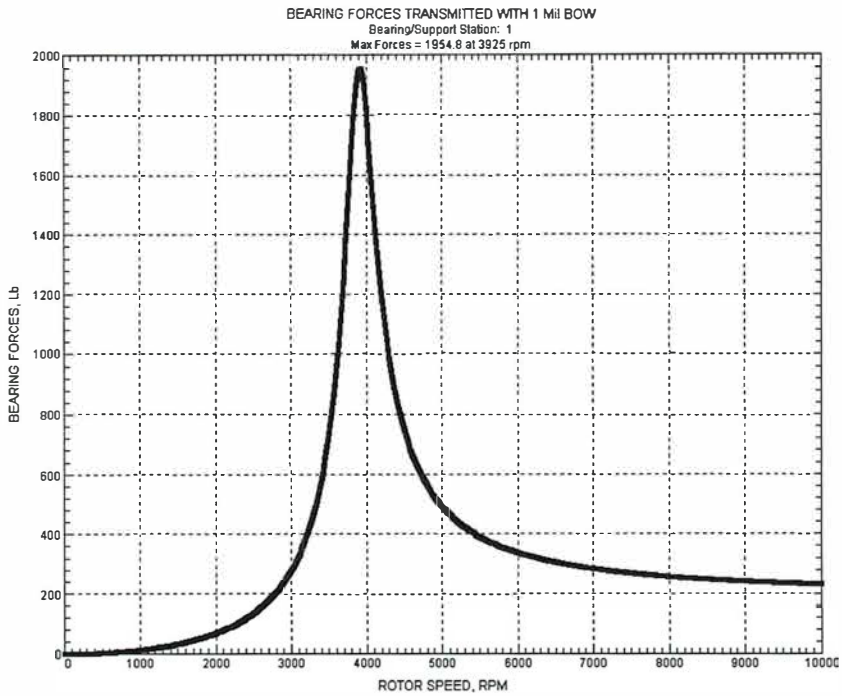

Figure 2.5-4 Bearing Forces Transmitted With 1 Mil Shaft Bow

The bearing forces as shown in Fig 2.5-4 are zero at low speed and reach a peak at the critical speed. As the speed increases, although the rotor amplitude approaches zero as the speed increases, the bearing forces do not. This is because the initial shaft bow causes a bearing reaction due to the bow vector being straightened out. The high speed bearing forces transmitted is in direct relationship to the initial bow and the shaft stiffness as follows:

$$F_{brg}\Big|_{N\to\infty} = \frac{K_s \delta_{bow}}{2} \qquad (2.5\text{-}6)$$

$$\textit{Where} \quad K_s = \frac{48EI}{L^3} \quad ; \quad I = \frac{\pi D^4}{64}$$

Example 2.5-1 Bearing Force Estimate At High Speed And At The Critical Speed

Consider the Jeffcott rotor of Fig 2.2-1. The shaft characteristics are as follows:

$$L_s = 72\,in \;;\; D_s = 6.6\,in \;;\; E = 30.0\times10^6\; Lb/in$$

$$I = \frac{\pi D_s^4}{64} = 93.1\,in^4 \;;\; K_S = \frac{48EI}{L_s^3} = 359{,}162\; Lb/in$$

The bearing force at high speed is :

$$F_{brg\,f\to\infty} = \frac{K_s \delta_r}{2} = \frac{359{,}162\times0.001}{2} = 178\; Lb$$

The bearing force at the critical speed is approximately

$$F_{brg\,f=1} = A_{cr} \times F_{brg\,f\to\infty} = 10\times178 = 1{,}780\; Lb$$

From the above example, it is seen that although the rotor amplitude due to shaft bow reduces to zero as the speed exceeds the critical speed, the bearing forces do not. The high speed bearing forces are approximately equal to the product of the initial shaft bow times the shaft stiffness value. Fig. 2.5-4 shows the bearing forces approaching 200 Lb at 10,000 RPM as compared to the approximate value of 178 Lb as calculated above.

The maximum bearing force transmitted at the critical speed with the 1 mil shaft bow is 1955 Lb as shown in Fig. 2.5-4. This value should be compared to the computed maximum bearing force of 1935 Lb as shown in Fig. 2.4-11 for the unbalanced rotor in which the modal unbalance eccentricity (12.8 oz-in) is 1 mil. Although the speed dependent response coefficients are different for radial unbalance and shaft bow, it is seen that at the critical speed, the response and bearing forces transmitted have similar effects.

Response With $\delta_r/e_u = 0.5$ At 90^0 Lag To Unbalance

Fig. 2.5-5 represents a cross section of the Jeffcott rotor taken at the disk location. The rotor unbalance eccentricity vector e_u is directed along the relative X axis. The keyphaser mark on the shaft determines the relative X axis. The timing mark on the shaft is shown lined up with the absolute X axis. The shaft is directed along the Z axis, forming a right handed coordinate system. The relative Y axis attached to the shaft is positive in the direction of rotation.

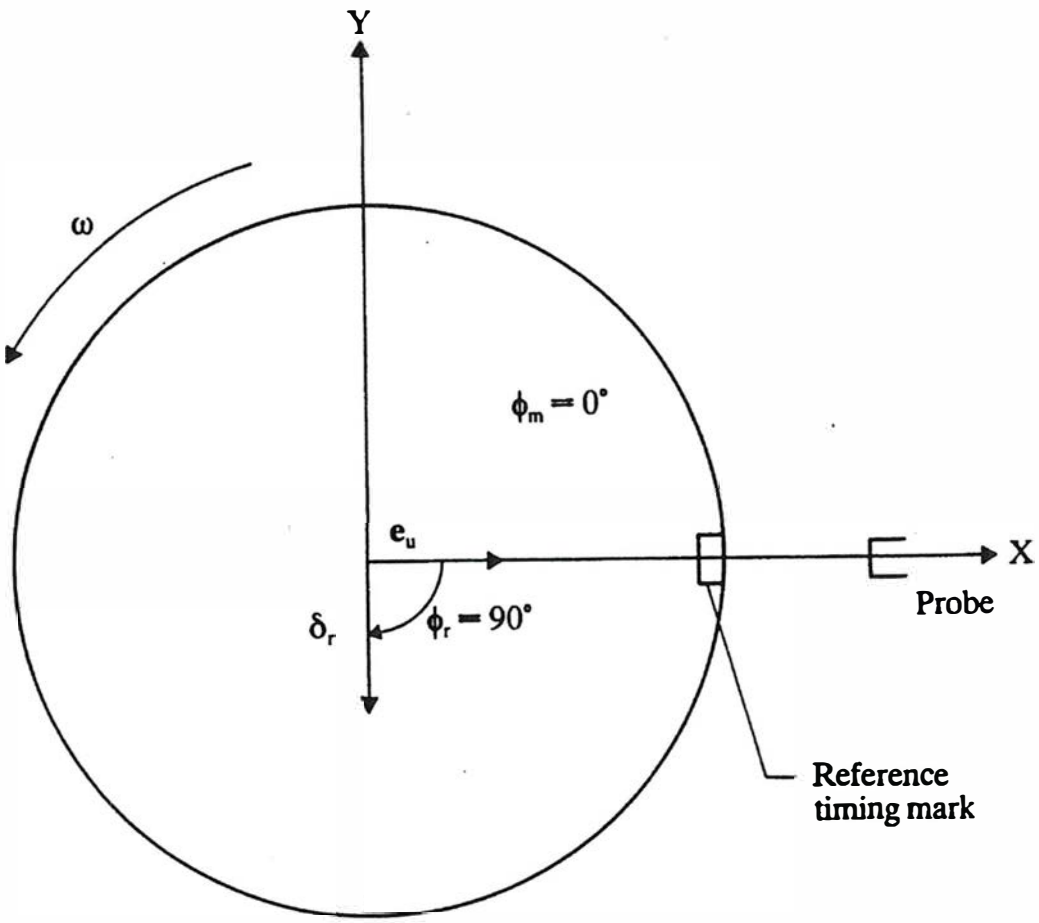

Figure 2.5-5 Rotor Cross Section Showing Relative Positions Of Unbalance Eccentricity Vector e_u And Shaft Bow δ_r

The rotor unbalance and shaft bow components are specified with respect to the relative X,Y axes attached to the shaft. In Fig. 2.5-5, the bow vector δr is shown drawn at the lag angle of $\Phi_r = 90^0$. The unbalance eccentricity vector e_u is shown drawn with the lag angle of $\Phi_m = 0^0$. The unbalance is specified as lying along the direction of the timing mark or keyphaser.

Since the unbalance eccentricity vector and shaft bow have the same influence coefficients at the critical speed, the total response may be considered as the vector sum of the two components. Thus a small amount of shaft bow may exert a large unbalance response which is equivalent to the unbalance as follows:

$$U_{bow} = M_{modal} \times \delta_r \qquad (2.5\text{-}7)$$

Thus the response of the Jeffcott rotor at the critical speed with 1 mil shaft bow is equivalent to the unbalance response of 12.8 oz-in or 1 mil modal eccentricity at the critical speed.

Fig. 2.5-6 represents the response for a range of damping ratios in which the shaft bow is ½ of the rotor unbalance eccentricity and is lagging the unbalance vector by 90deg.

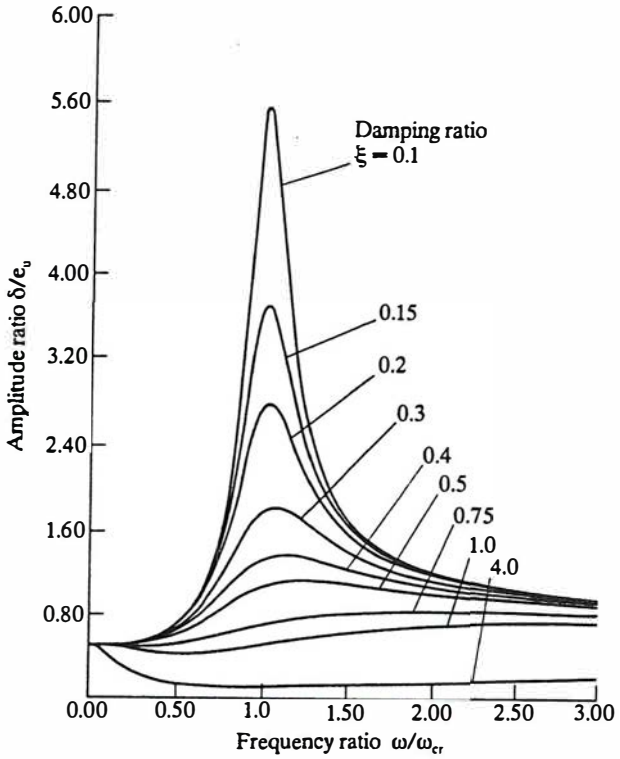

Fig. 2.5-6 Response Of Bowed Rotor With δr=0.5 , Φr = 90⁰

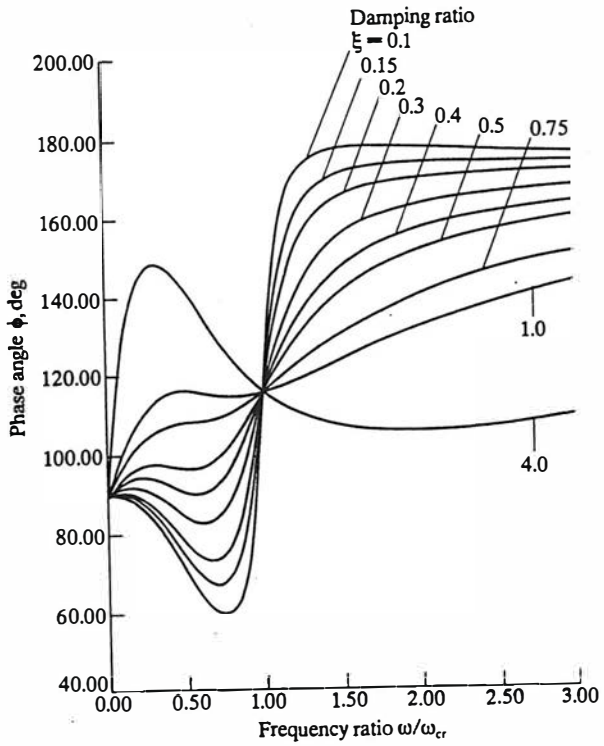

Fig. 2.5-7 Phase Angles Of Bowed Rotor With δr=0.5 , Φr = 90⁰

In Fig 2.5-6, the initial response is equal to the shaft bow. As the speed increases, the influence of unbalance begins to take effect. The amplitude at the critical speed is equal to the product of the rotor amplification factor times the sum of the unbalance eccentricity vector and the shaft bow vector. As the speed exceeds the critical speed, the rotor motion approaches the dimensionless unbalance eccentricity value of 1.

In Fig. 2.5-6, for a value of $\xi = 0.1$, the critical speed amplification factor is $A_{cr} = 5$. For the case of dimensionless unbalance of e_u=1.0, the dimensionless amplitude at the critical speed, at $f = 1$ would be 5. The effective excitation unbalance eccentricity is given by:

$$e_{eff} = \sqrt{\left(e_u \cos\phi_m + \delta_{rx}\right)^2 + \left(-e_u \sin\phi_m + \delta_{ry}\right)^2} = \sqrt{1 + 0.5^2} = 1.12$$

$$A_{critical\ speed} = 1.12 \times 5 = 5.6 \qquad (2.5\text{-}7)$$

If the shaft bow vector is within 120 deg of the unbalance eccentricity vector, then the response will be increased. Beyond 120deg separation, the 2 effects will start to cancel each other out. This leads to balancing procedures of shaft bow with unbalance corrections placed out of phase to the bow vector. Fig 2.5-7 shows the phase relationship. Notice that it is possible to have a reversal in phase as speed increases due to the influence of shaft bow.

Response With Bow Vector At 180^0 Out Of Phase To Unbalance

Fig. 2.5-8 represents the rotor response in which the bow vector $\delta_r/e_u = 0.5$. The relative bow vector is half of the unbalance eccentricity vector and out of phase to the unbalance. In this case the rotor amplitude goes to zero at 70% of the critical speed. At this speed, the influences of shaft bow and unbalance are equal and out of phase.

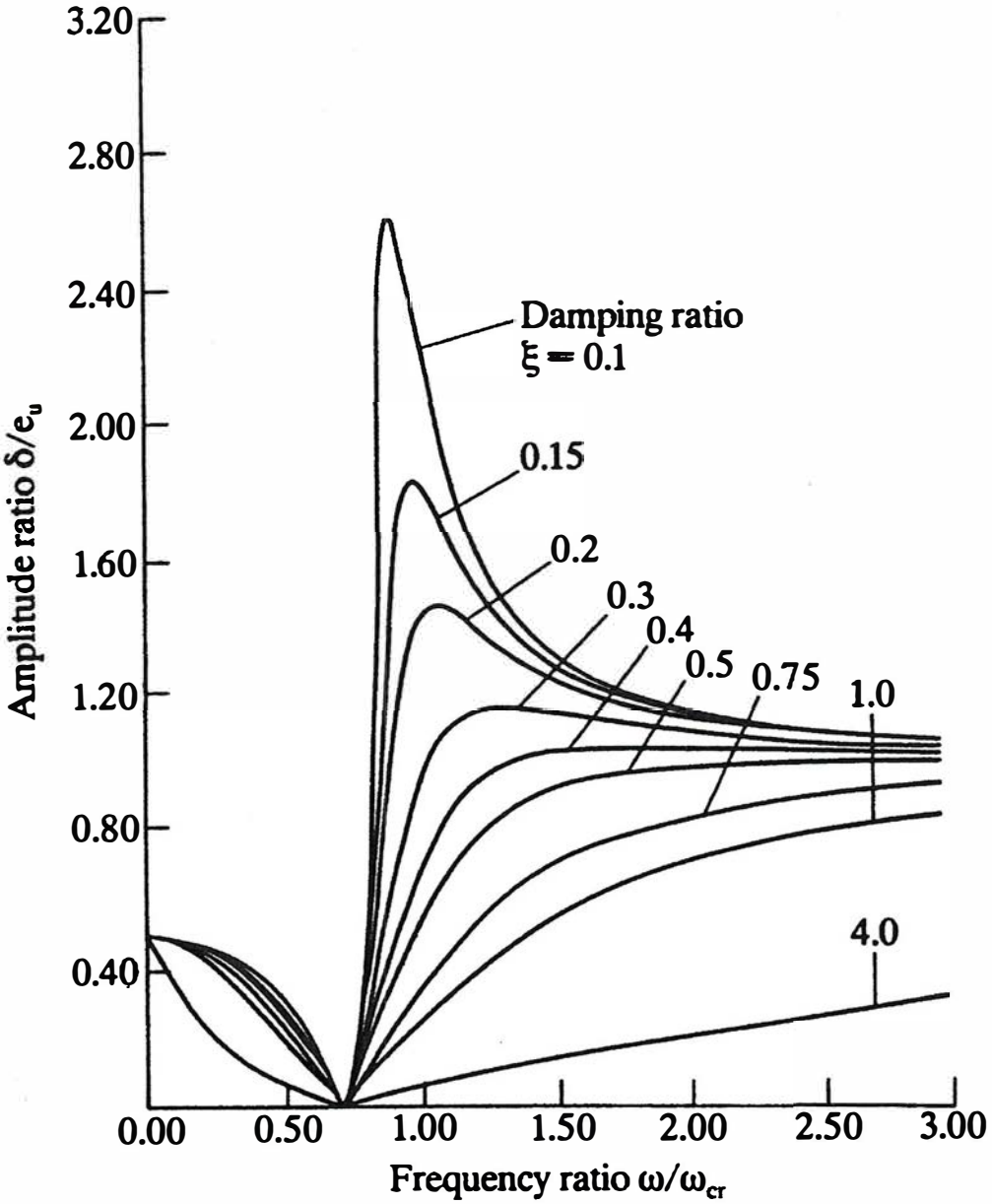

Figure 2.5-8 Response With Dimensionless Shaft Bow 0f 0.5 Out Of Phase To The Unbalance

At very high speeds, the amplitude will approach 1 which represents the dimensionless unbalance eccentricity value. Fig. 2.5-9 is similar to Fig. 2.5-8 except that the shaft bow is now twice the unbalance eccentricity vector. In this case, the influence of shaft bow and unbalance are equal and of opposite signs at a speed of 141% of the critical speed. In Fig. 2.5-10, the shaft bow is of equal value to the unbalance eccentricity vector but 180^0 out of phase. In this case the rotor amplitude is zero exactly at the critical speed.

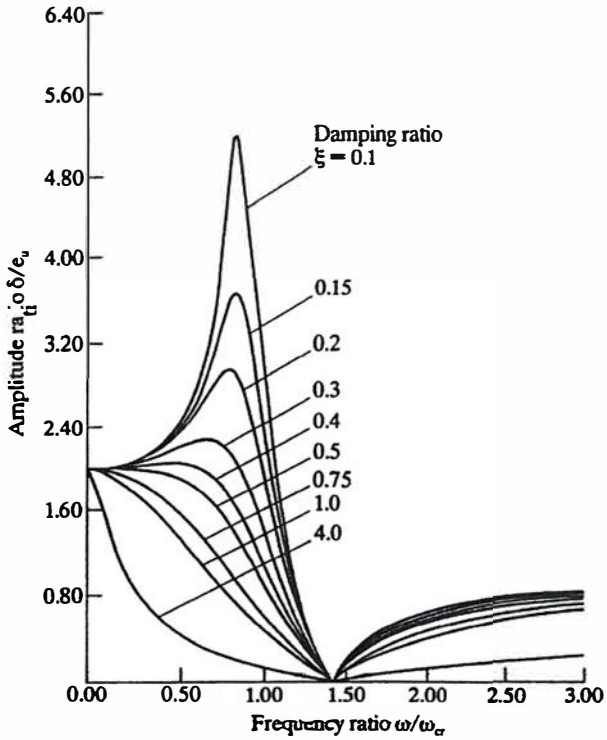

Fig. 2.5-9 Response With Dim. Shaft Bow Of 2 Out Of Phase To Unbalance

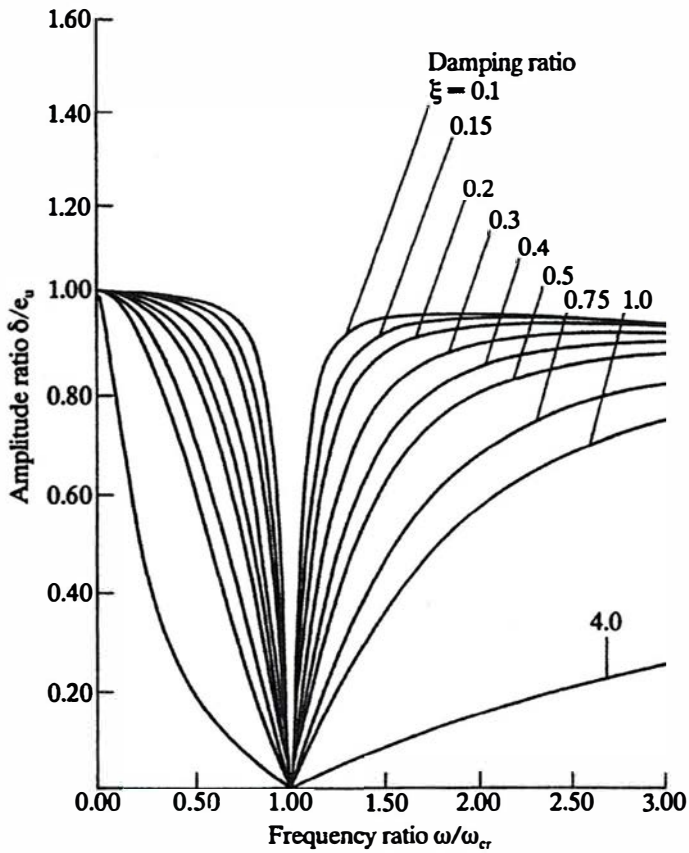

Fig. 2.5-10 Shaft Bow Equal To And Out Of Phase To Unbalance - Balanced Condition

Jeffcott Simulation Of Industrial Compressor With Shaft Bow And Unbalance

Fug 2.5-11 represents the unbalance response of a multistage compressor in tilting pad bearings. From the comparison of Fig. 2.5-11 to Fig 2.5-9, it can be seen that the rotor has shaft bow as well as unbalance.

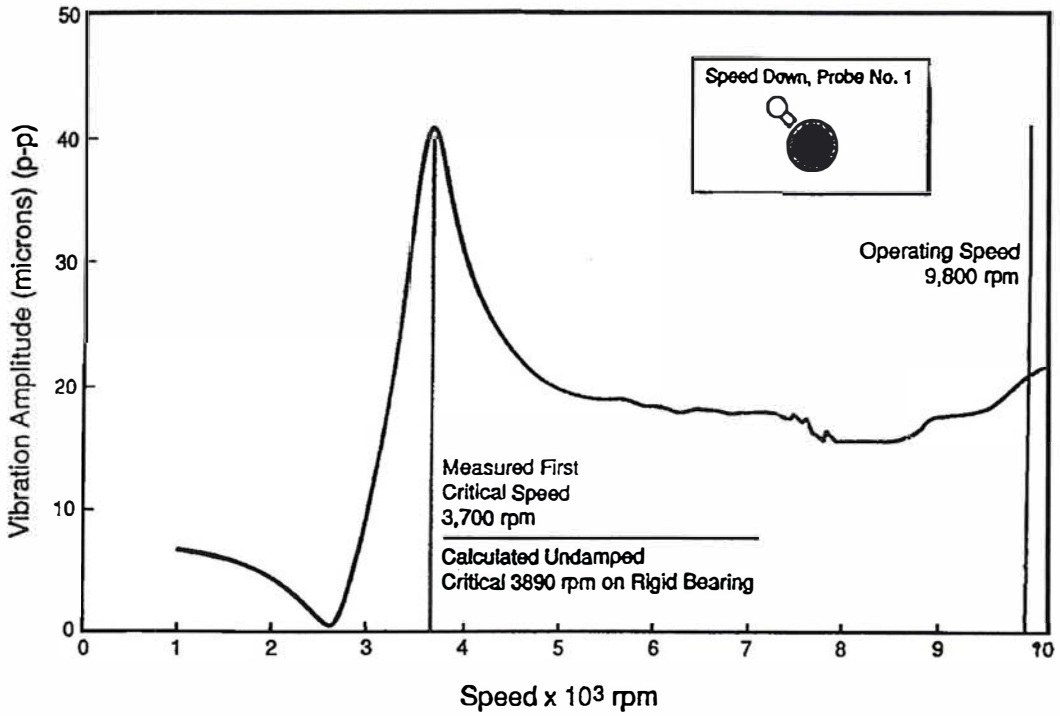

Figure 2-5-11 Response of 6 Stage Compressor With Shaft Bow And Unbalance
(*Allaire 1992*)

From Fig. 2.5-11, as recorded by Allaire, it is apparent that, in addition to rotor unbalance, the rotor also has shaft bow. The amount of shaft bow is approximately one-half of the modal unbalance eccentricity vector. Since the rotor amplitude approaches zero near 2700 RPM, the bow is out of phase to the unbalance vector. After the critical speed is reached at 3700 RPM, the rotor amplitude reduces to the 1st modal unbalance eccentricity. Above 7000 RPM the rotor motion begins to increase slightly due to the influence of the second mode.

Simulation Using DYROBES

The response of the 6 stage compressor may be simulated by the Jeffcott rotor model using equivalent modal parameters to simulate the rotor response through the first critical speed. In the previous jeffcott model, the center span damping was doubled to represent the more highly damped compressor. A shaft bow vector of .5 mils at zero deg was assumed. The unbalance vector was assumed to be acting at 178^0 Since the bow vector is approximately one-half the modal unbalance eccentricity vector, the minimum response approaching zero will be at 70% of the critical speed.

Fig. 2-5-12 represents the rotor amplitude of the simulated 6 stage compressor with a small bow and the unbalance eccentricity of twice the magnitude but out of phase.

Jeffcott Simulation Of Industrial Compressor With Shaft Bow And Unbalance

Fig. 2.5-12 represents the simulated motion of the 6 stage compressor using ***DYROBES*** with shaft bow in the Jeffcott model along with center plane rotor unbalance.

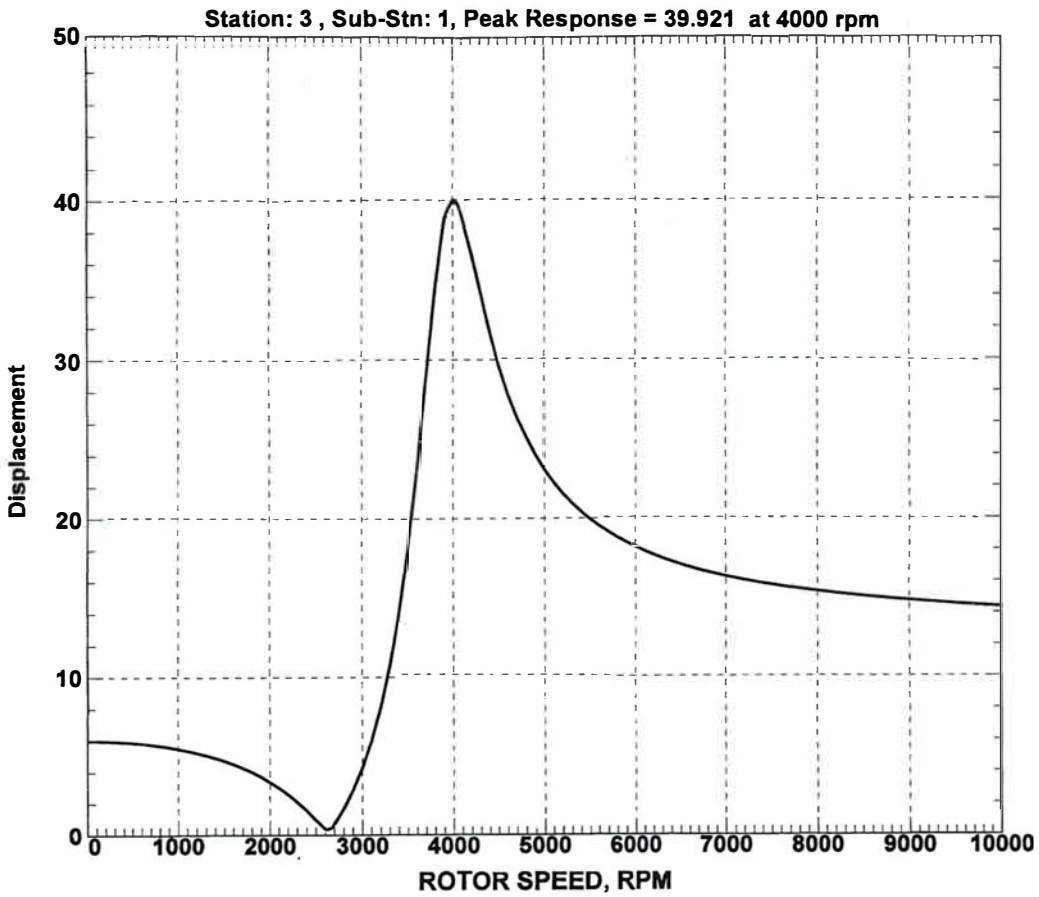

Figure 2.5-12 Jeffcott Model Simulation of 6 Stage Compressor Response With Shaft Bow And Out Of Phase Unbalance

In this case Jeffcott rotor properties of mass, stiffness, and damping represent the multistage compressor first modal properties. The modal unbalance eccentricity vector is twice as large as the shaft bow and is out of phase to the bow. Since the unbalance is larger then the bow the motion approaches zero below the critical speed. The local self balancing speed of zero amplitude is proportional to the square root of the ratio of bow divided by the modal unbalance eccentricity vector times the critical speed as follows.

$$N_{local\ balance} = \sqrt{\frac{\delta_{bow}}{e_u}} \times N_{critical\ speed} \qquad (2.5\text{-}9)$$

The rotor appears to be balanced at the low speed of 2,800 RPM which is below the first critical speed. At this speed, the two effects cancel each other out. The rotor is not correctly balanced. Measurements for field balancing the compressor should include readings above the first critical speed as well as below it if a least squared error balancing program is used.

Phase Relationship With Shaft Bow And Out Of Phase Unbalance

Fig 2.5-13 represents the phase change with the combination of shaft bow and unbalance

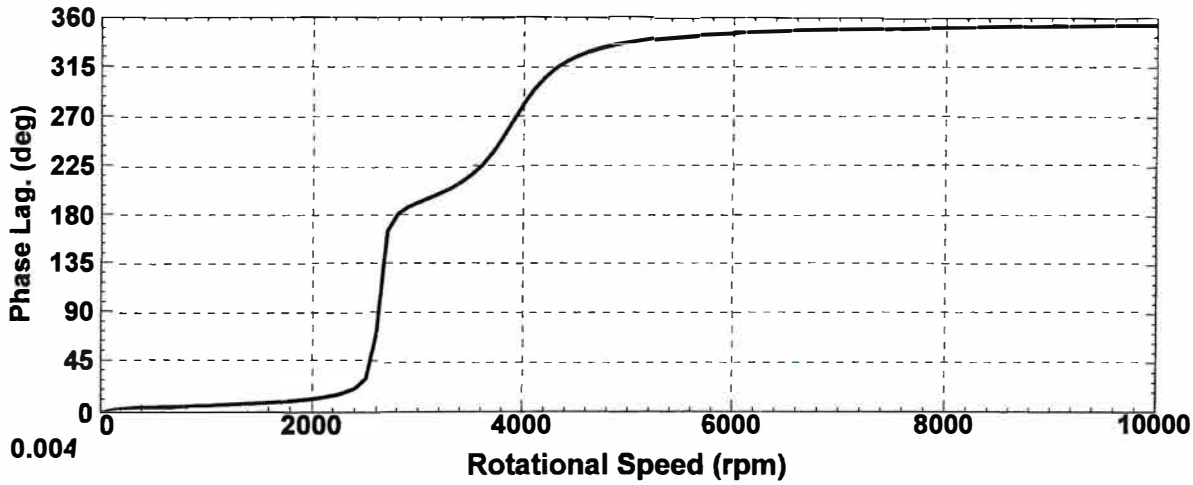

Figure 2.5-13 Phase Angle Change With Small Shaft Bow And Out of Phase Unbalance

Fig. 2.5-14 represents the polar plot of the synchronous response with bow and unbalance.

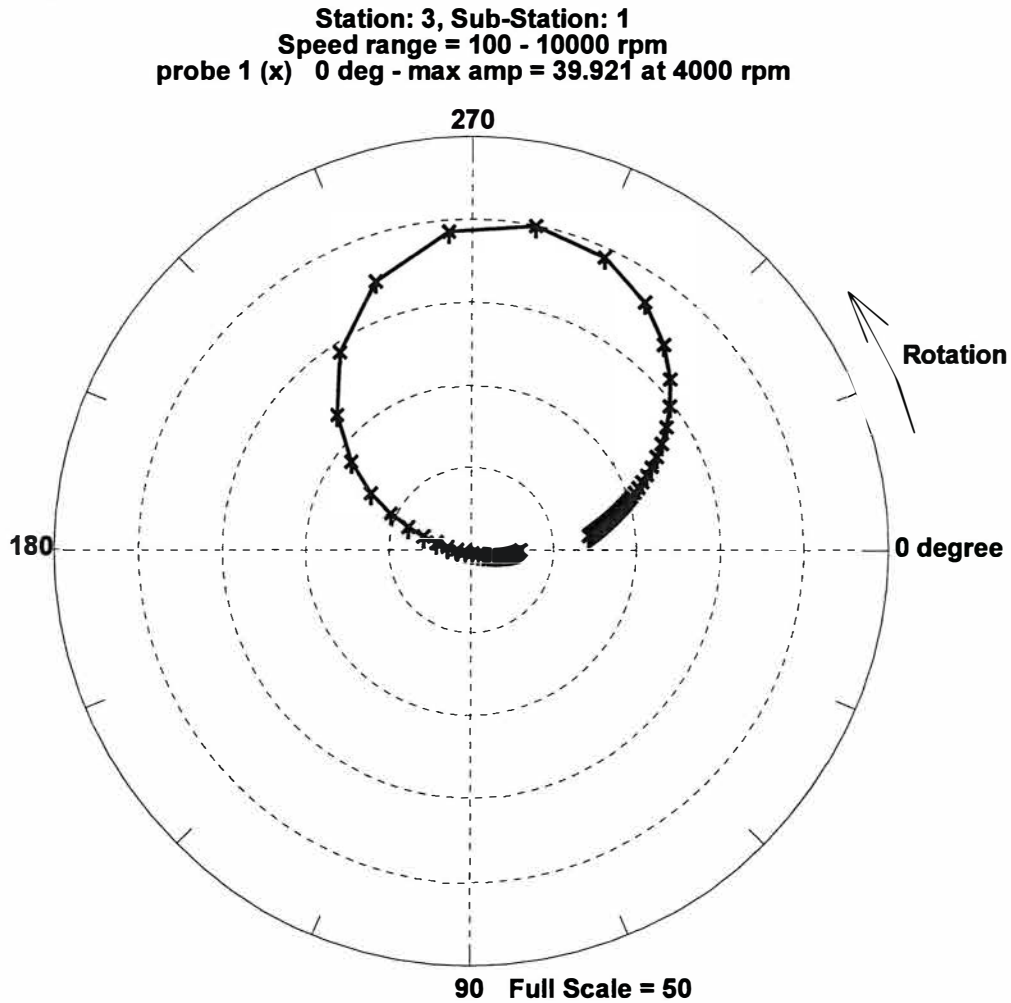

Figure 2.5-14 Polar Plot Of Rotor Motion With Small Bow And Unbalance Out of Phase

Phase Response With Various Bow δ_r And Unbalance e_u Values

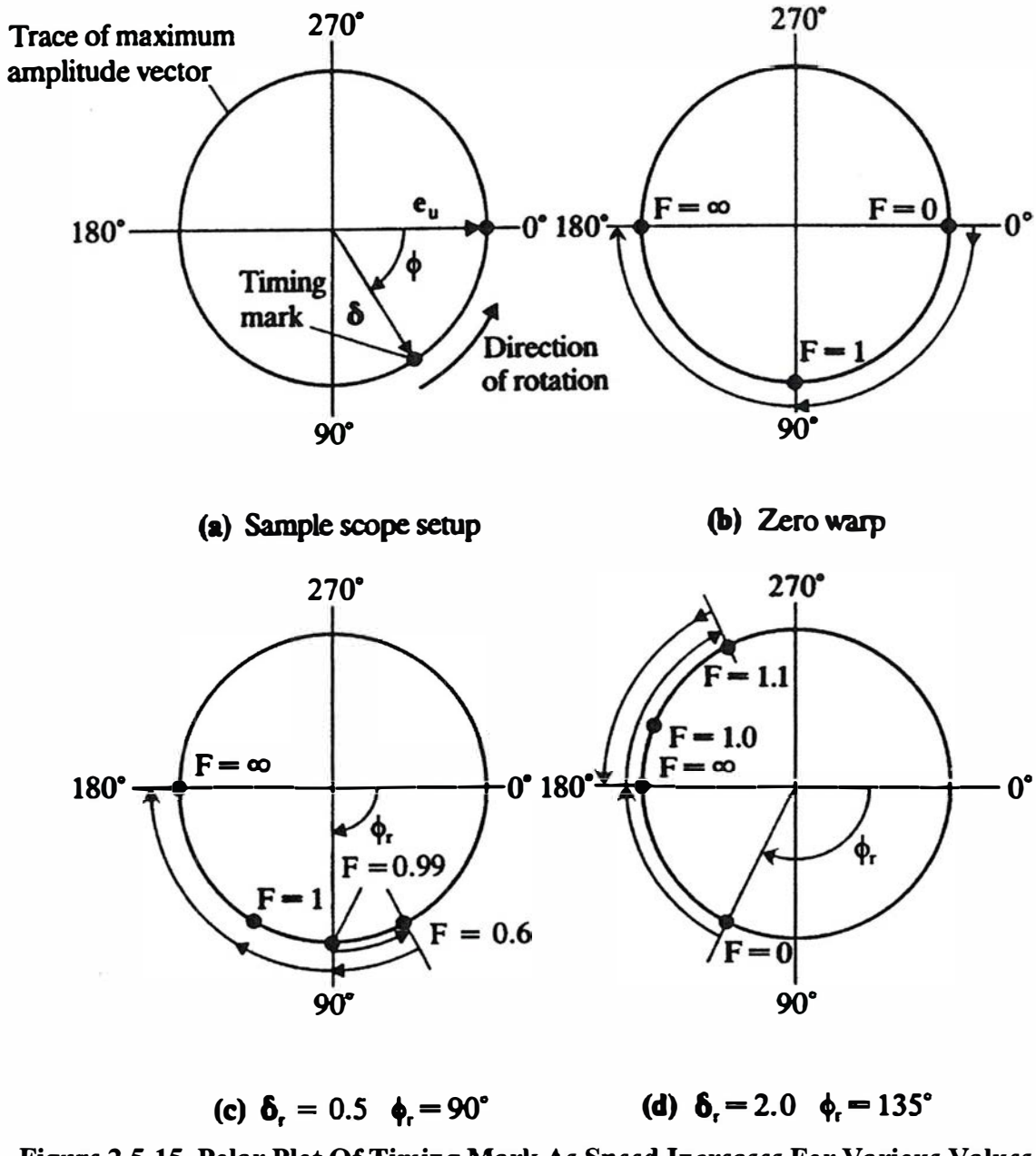

Figure 2.5-15 Polar Plot Of Timing Mark As Speed Increases For Various Values Of Shaft Bow δ_r And Unbalance Eccentricity e_u ***(Nicholas et al., 1976)***

Fig. 2.5-15 represents the change in the timing reference mark as speed changes for various combinations of shaft bow and unbalance. In **Fig.(a)** ,we have the conventional change from 0 to 180^0 as would be expected for the Jeffcott rotor. **Fig 2.5-13** shows a 180^0 shift at 2700 RPM which is not the critical speed ot the rotor. The phase then continues to increase to 360^0 due to the combination of bow and out of phase unbalance.

Normally, with conventional unbalance we would see the timing mark moving smoothly against rotation. However, when shaft bow is present, a reversal in the phase at some speed may occur depending on the bow magnitude and relative phase. For example in **(c)**, the shaft bow is ½ of e_u. The phase reverses until a speed of 60% of the critical speed is reached.

3 EXTENDED JEFFCOTT ROTOR

3.1 Description of Extended Jeffcott Rotor

Figure 3.1-1 represents the single mass Jeffcott rotor mounted on flexible damped supports. This model is often referred to as the extended Jeffcott Rotor. The generalized Jeffcott rotor is the natural and logical extension of the original Jeffcott rotor on simple supports. At the time H.H. Jeffcott performed his analysis, it would have not been possible to evaluate a more complex model. Also, the concept of bearing or support stiffness and damping properties was not developed at this time.

The extended Jeffcott model as shown in Figure 3.1–1 was taken from the book "***Rotating Machinery Vibrations***", *Marcel Dekker*, 2001, pg 34 by Dr. Mike Adams. In his representation of the extended Jeffcott rotor, he shows a system of 8 degrees of freedom. These degrees of freedom represent the 6 horizontal and vertical displacements of the bearings and center span disk plus 2 additional degrees of freedom to represent the disk conical motion. In Fig. 3.1-1, the disk rotational degrees of freedom are not included as this leads to higher order modes of motion involving the gyroscopic moments acting on the disk. The subject of disk gyroscopic effects will be treated in Chapter 4.

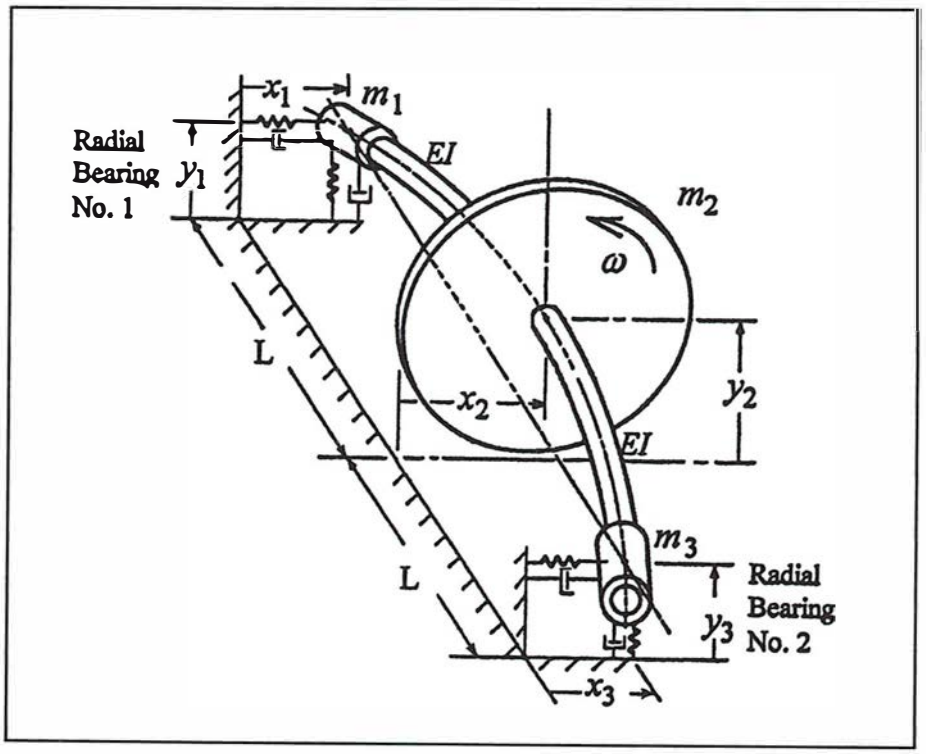

Figure 3.1-1 Jeffcott Rotor On Flexible Supports

The disk angular coordinates are required to represent the disk gyroscopic moments. The inclusion of the disk gyroscopic moments creates a higher conical mode of motion in which the disk mass center is a node point. In general this second mode is well above the normal operating speed of the Jeffcott rotor first mode and is not likely to be encountered .

From the standpoint of understanding the behavior of the extended Jeffcott rotor on flexible supports, the gyroscopic moments are not required and hence will be neglected in this Chapter. For the first mode, for example, the disk moves in a plane and hence there are no gyroscopic moments exerted on the disk. The extended Jeffcott rotor is reduced to a system of 6 degrees of freedom. These degrees of freedom are 3 in the x direction and y direction as shown in Fig 3.1-1. The bearings are considered as simple springs and dampers. At this point, only the direct bearing stiffness and damping coefficients will be considered.

3.2 Jeffcott Rotor Equations of Motion On Flexible Supports

General Equations Of Motion

The extended Jeffcott rotor equations of motion without gyroscopic coupling are expressed as following:

$$\begin{bmatrix}[M] & \\ & [M]\end{bmatrix}\begin{Bmatrix}\{\ddot{X}\}\\ \{\ddot{Y}\}\end{Bmatrix}+\begin{bmatrix}[C_{xx}] & [C_{xy}]\\ [C_{yx}] & [C_{yy}]\end{bmatrix}\begin{Bmatrix}\{\dot{X}\}\\ \{\dot{Y}\}\end{Bmatrix}+$$
$$+\begin{bmatrix}[K_s] & \\ & [K_s]\end{bmatrix}\begin{Bmatrix}\{X\}\\ \{Y\}\end{Bmatrix}+\begin{bmatrix}[K_{xx}] & [K_{xy}]\\ [K_{yx}] & [K_{yy}]\end{bmatrix}\begin{Bmatrix}\{X\}\\ \{Y\}\end{Bmatrix}=\begin{Bmatrix}F_x(t)\\ F_y(t)\end{Bmatrix} \qquad (3.2\text{-}1)$$

The above generalized matrix equations of motion are applicable to a multimass flexible rotor without the explicit representation of the disk gyroscopic moments.

System Mass Matrix

For mass matrix M as applied to the extended Jeffcott rotor, we have the following:

$$[M]=\begin{bmatrix}M_1 & & \\ & M_2 & \\ & & M_3\end{bmatrix}=\begin{bmatrix}\frac{m_{shaft}}{4} & & \\ & \frac{m_{shaft}}{2}+M_{disk} & \\ & & \frac{m_{shaft}}{4}\end{bmatrix} \qquad (3.2\text{-}2)$$

For the case of the extended Jeffcott rotor, we have ½ of the shaft mass placed along with the disk mass at the rotor center at station 2. The effective mass acting at each bearing station is 1/4 of the total shaft mass. For the case of the conventional Jeffcott rotor in which the bearings are constrained, we are reduced to the center plane mass M_2 equal to the sum of the disk weight plus one-half of the shaft weight. For the case of a multistage compressor, the equivalent center span mass will correspond to the rotor 1st modal mass computed with constrained bearings.

System Damping Matrix

The damping matrix C for the extended Jeffcott rotor for this analysis will consist of symmetrical bearing damping coefficients for both the x and y directions. The center span damping coefficient C_2 will be considered as small in comparison to the bearing damping coefficient C_b. The bearing cross coupling coefficients C_{xy} and C_{yx} will be ignored. The bearing model to be considered will be similar to a 4 pad tilting pad bearing configuration with load between pads. The damping matrices for the x and y directions will be uncoupled and symmetric as follows:

$$[C_{xx}]=[C_{yy}]=\begin{bmatrix} C_b & & \\ & C_2 & \\ & & C_b \end{bmatrix} \qquad (3.2\text{-}3)$$

In general, we assume that the total bearing damping is much greater than the center span damping, or that

$$2C_b > C_2 \qquad (3.2\text{-}4)$$

What we are interested in is the total effective modal damping for the extended Jeffcott rotor on flexible supports. The effective modal damping is the sum of the conversion of bearing damping plus the center span damping as follows:

$$C_{modal}=2C_b \times C_f + C_2 \qquad (3.2\text{-}5)$$

It is desirable to make the modal damping as high as possible. It will be shown later that the total effective modal damping is dependent upon both the bearing damping values and the bearing to shaft stiffness ratio.

Thus for a rigid rotor the effective modal damping is given by:

$$C_{modal-rigid\ rotor}=2C_b+C_2 \qquad (3.2\text{-}6)$$

For the case of either high bearing damping or high bearing stiffness, the modal damping converges to C_2, the center span damping. Thus, in this case, we have lost all beneficial effects of the bearings. It will be shown, that under these circumstances, the rotor will become very sensitive to self excited whirl instabilities and will have a very high amplification factor at the first critical speed.

$$C_{modal-rigid\ bearings}=2C_b \cdot \varepsilon + C_2 \Rightarrow C_2 \qquad (3.2\text{-}7)$$

Here we see the paradox that even with very high bearing damping present in the rotor that very little of it may be converted to effective modal damping. The rotor amplification factor at the 1st critical speed will be given by:

$$A_c = \frac{M_{modal}\,\omega_c}{C_{modal}} \qquad (3.2\text{-}8)$$

Shaft Stiffness Matrix

The stiffness matrix is composed of two matrices. The first matrix is the symmetric and singular shaft stiffness $[K]_s$ matrix. This matrix may be derived from finite element methods or simply by applying first principles of structural mechanics. The second matrix, $[K]_b$ consists of the bearing coefficients acting at the three stations.

The properties of the shaft stiffness matrix are as follows:

The stiffness matrix is symmetrical
The matrix is singular of order 2
The matrix is positive definite
When the bearings are constrained, the center term is equal to K

The unrestrained stiffness matrix is singular and has no strain energy for rigid body cylindrical and conical modes of motion. Hence we have the two conditions on strain energy such that

$$V_1 = \Phi_1^T [K]_s \Phi_1 = 0$$
$$\textit{Where } \Phi_1^T = [1 \quad 1 \quad 1]$$
$$\textit{and} \qquad (3.2\text{-}9)$$
$$V_2 = \Phi_2^T [K]_s \Phi_2 = 0$$
$$\textit{Where } \Phi_2^T = [1 \quad 0 \quad -1]$$

The shaft stiffness matrix can be shown to be represented as follows:

$$[K]_s = \begin{bmatrix} \frac{K}{4} & -\frac{K}{2} & \frac{K}{4} \\ -\frac{K}{2} & K & -\frac{K}{2} \\ \frac{K}{4} & -\frac{K}{2} & \frac{K}{4} \end{bmatrix} \qquad (3.2\text{-}10)$$

It is seen that the determinant of the above stiffness matrix is singular. If one multiplies the rows by the rigid body cylindrical mode shape of $\{1 \;\; 1 \;\; 1\}^T$, then it is seen that the resulting vector is the null vector. The similar situation is obtained when the shaft stiffness matrix is multiplied by the rigid body conical mode of $\{1 \;\; 0 \;\; -1\}^T$. In order to obtain the original stiffness value of the Jeffcott rotor on simple supports, we zero out the first and third rows and columns of the 3x3 stiffness matrix. When this is performed, we are left with uncoupled equations of motion for the x and y directions.

Equations of Motion With Symmetric Bearings

The equations of motion in the x and y directions are uncoupled due to the absence of bearing cross coupling or aerodynamic cross coupling acting at the rotor center. The x and y equations may be separately written as follows:

$$[M]\{\ddot{X}\}+[C]\{\dot{X}\}+[K]\{X\}=\omega^2\{U\}\cos(\omega t-\varphi)$$
$$[M]\{\ddot{Y}\}+[C]\{\dot{Y}\}+[K]\{Y\}=\omega^2\{U\}\sin(\omega t-\varphi) \qquad (3.2\text{-}11)$$

Where:

$$[M]=\begin{bmatrix}\frac{M_s}{4} & & \\ & \frac{M_s}{2}+M_d & \\ & & \frac{M_s}{4}\end{bmatrix} \quad ; \quad [C]=\begin{bmatrix}C_b & & \\ & 0 & \\ & & C_b\end{bmatrix}$$

And

$$[K]=\begin{bmatrix}K_b+\frac{K}{4} & -\frac{K}{2} & \frac{K}{4} \\ -\frac{K}{2} & K & -\frac{K}{2} \\ \frac{K}{4} & -\frac{K}{2} & K_b+\frac{K}{4}\end{bmatrix}$$

In the current model, we will assume that the center span damping is small in comparison to the bearing damping and may be ignored. However, this is not always the case as a small amount of center plane damping has significant effects in actual rotors with stiff bearings and often may not be ignored.

Since the [M], [C], and [K] matrices are symmetric, the {x} and {y} equations of motion may be expressed in complex form as follows:

$$\{Z\}=\{X\}+i\{Y\} \qquad (3.2\text{-}12)$$

The complex vector {z} may be viewed as a 2 dimensional vector representing the rotating or whirling motion of the shaft at the 3 distinct stations. The use of the complex vector to represent both the horizontal and vertical motions of the shaft is most effective for the case of symmetrical rotor and bearing properties.

The equations of motion using the complex vector {z} is given by:

$$[M]\{\ddot{Z}\}+[C]\{\dot{Z}\}+[K]\{Z\}=\omega^2\{U\}e^{i\omega t-\varphi} \qquad (3.2\text{-}13)$$

The homogenous solution may be solved for the damped eigenvalues or the steady state solution may be solved to determine the synchronous response due to unbalance. Both methods may be used to determine the optimum bearing damping for a given bearing stiffness. The damped eigenvalues will determine the maximum log decrement for the first forward mode. The forced response will determine the lowest possible amplification factor.

3.3 Damped Eigenvalue Analysis

General Eigenvalue Problem

The damped natural frequencies of the system may be determined from the homogeneous equations of motion without the application of the rotor forcing functions such as unbalance. The displacement vector {x} is a assumed to be of the general form:

$$\{X(t)\} = \{X\}e^{\lambda t} \qquad (3.3\text{-}1)$$

Where λ_i is the i_{th} complex eigenvalue $= p_i + i\,\omega_{di}$

And p = real root $= -\xi\omega_c$

$$\xi = \frac{c}{c_c}\ ;\ C_c = 2M\omega_c$$

ω_{di} = i_{th} damped natural frequency

$$= \omega_c\sqrt{1-\xi^2}$$

The substitution of Eq *(3.3-1)* into Eq *(3.2-13)*, neglecting the forcing function, results in the following eigenvalue problem

$$\left[\lambda^2[M]+\lambda[C]+[K]\right]\{X\} = 0 \qquad (3.3\text{-}2)$$

Characteristic Polynomial

Since the components of the {X} vector are in general not all zero or null, the determinant of the following matrix must vanish.

$$\left|\lambda^2[M]+\lambda[C]+[K]\right| = 0 \qquad (3.3\text{-}3)$$

This leads to the characteristic eigenvalue problem as follows:

$$\lambda^n + a_1\lambda^{n-1} + a_2\lambda^{n-2} + \cdots + a_n = 0 \qquad (3.3\text{-}4)$$

The coefficients $a_1 \Rightarrow a_n$ are called the invariants of the characteristic equation. The first invariant or coefficient a_1 is equal to the sum of the eigenvalues as follows:

$$a_1 = -(\lambda_1 + \lambda_2 + \lambda_3 \cdots \lambda_n) \qquad (3.3\text{-}5)$$

The n^{th} invariant of the characteristic polynomial is equal to the product of the eigenvalues.

$$a_n = \lambda_1\lambda_2\lambda_3\cdots\lambda_n = \prod_{i=1}^{n}\lambda_1 \qquad (3.3\text{-}6)$$

For the equations of motion as given by Eq *(3.2-13)*, in which the x and y directions of motion are uncoupled, the eigenvalue problem for each direction may be computed separately. For the extended Jeffcott rotor with 3 mass stations, the characteristic equation is of order 6.

If the equations are coupled due to aerodynamic or bearing effects, the equation is of order 12. Even the 12 th order equation presents numerical difficulties in root extraction.

Numerical Difficulties With Characteristic Polynomial

The coefficients of the characteristic polynomial increase in magnitude. This leads to considerable numerical difficulties in computing the complex eigenvalues for high order systems. Eq. *(3.3-5)* for the first invariant is equal to the sum of the eigenvalues. The nth or last invariant is equal to the product of all the eigenvalues. If we take the ratio of the nth coefficient divided by the first coefficient, we obtain the following ratio.

$$R_{a_n/a_1} = \frac{\prod_{i-1}^{n} \lambda_i}{\sum_{i=1}^{n} \lambda_i} \approx \lambda_1 \lambda_2 \lambda_3 \ldots \lambda_{n-1} \qquad (3.3\text{-}7)$$

Thus we see that the magnitude of the n th coefficient may be of a much higher order of magnitude higher than the first coefficient. This presents a problem in eigenvalue extraction, even for systems in which scaling is employed in generating the characteristic polynomial. Even the simple case of the generalized Jeffcott rotor presents problems in accurate eigenvalue extraction of the roots for the 12^{th} order equation. Problems are encountered even when scaling of the coefficients is employed. Thus we see that attempts to determine stability of multimass rotor systems by root extraction from a large system polynomial is not recommended due to the numerical difficulties encountered with the generation of accurate roots.

Matrix Reduction of Extended Jeffcott Rotor With Symmetrical Bearings

When the bearings are symmetrical in the x and y directions and both bearings are identical, then the matrix representation may be further reduced. At this point we are interested in determining the optimum damping for the bearings to maximize the system 1^{st} forward mode log decrement δ. Since we are not considering bearing cross coupling, and we are assuming that the motion of both bearings is identical, we may further reduce the matrix equations of motion from 3x3 to 2x2. The reduction of the equations of motion is accomplished by the following transformation. The assumption of the motion being equal at both bearings leads to the transformation matrix as follows:

$$\begin{Bmatrix} X_1 \\ X_2 \\ X_3 \end{Bmatrix} = [T]\{\bar{X}\} = \begin{bmatrix} 1 & 0 \\ 0 & 1 \\ 1 & 0 \end{bmatrix} \begin{Bmatrix} X_1 \\ X_2 \end{Bmatrix} \qquad (3.3\text{-}8)$$

The 3x3 equations of motion may be reduced to 2x2 by thr use of the above transformation equations as follows:

$$[T]^T \left[\lambda^2[M] + \lambda[C] + [K]\right][T] = 0 \qquad (3.3\text{-}9)$$

The resulting reduced matrix equations of motion for the symmetric Jeffcott rotor yields:

$$\lambda^2 \left[\bar{M}\right]_{2x2} + \lambda \left[\bar{C}\right]_{2x2} + \left[\bar{K}\right]_{2x2} = 0 \qquad (3.3\text{-}10)$$

Reduced Eigenvalue Problem For Extended Jeffcott Rotor

The reduced Jeffcott equations of motion in general form for the x direction, for example may be expressed by the following:

$$\begin{bmatrix} \frac{m_s}{2} & \\ & \frac{m_s}{2}+M_d \end{bmatrix}\begin{Bmatrix} \ddot{X}_1 \\ \ddot{X}_2 \end{Bmatrix}+\begin{bmatrix} 2C_b & 0 \\ 0 & 0 \end{bmatrix}\begin{Bmatrix} \dot{X}_1 \\ \dot{X}_2 \end{Bmatrix}+\begin{bmatrix} K+2K_b & -K \\ -K & K \end{bmatrix}\begin{Bmatrix} X_1 \\ X_2 \end{Bmatrix}= \\ =\omega^2\begin{Bmatrix} 0 \\ U_2 \end{Bmatrix}cos(\omega t-\phi_2) \qquad (3.3\text{-}11)$$

Since the amplitudes at the bearings at X_1 and X_3 are assumed to be smaller then the motion at the mass center, we have the situation that the kinetic energy of the Jeffcott rotor mass center is much larger than the sum of the kinetic energies of the bearing stations.

$$T_2=\frac{1}{2}M_2\dot{X}_2^2 \gg T_1+T_3=\frac{1}{2}\left(2\frac{M_s}{4}\right)\dot{X}_1^2 \qquad (3.3\text{-}12)$$

Thus a further reduction of the equations of motion and the characteristic equation may be obtained by ignoring the mass effects at the bearing locations. This leads to the following characteristic determinant:

$$\left|\lambda^2\begin{bmatrix} 0 & 0 \\ 0 & M_2 \end{bmatrix}+\lambda\begin{bmatrix} 2C_b & 0 \\ 0 & 0 \end{bmatrix}+\begin{bmatrix} K+2K_b & -K \\ -K & K \end{bmatrix}\right|=0 \qquad (3.3\text{-}13)$$

Collecting terms of the matrices and forming the determinant we have:

$$\begin{vmatrix} 2C_b\lambda+2K_b+K & -K \\ -K & M_2\lambda^2+K \end{vmatrix}=0 \qquad (3.3\text{-}14)$$

The expansion of the characteristic determinant leads to the following 3rd order equation.

$$2C_bM_2\lambda^3+M_2\left(K+2K_b\right)\lambda^2+2C_bK\lambda+2K_bK=0 \qquad (3.3\text{-}15)$$

The 3rd order characteristic polynomial will have the interesting behavior that the undamped system will reduce the polynomial to a second order system. This case will represent the undamped critical speed. This will be equivalent to the rotor on flexible supports. The added bearing flexibility will reduce the original critical speed. As the damping increases for a given bearing stiffness value, it will be seen that the damped critical speed will ***increase***. This is in marked contrast to the Jeffcott rotor with damping acting only at the center. In this case, the damped critical speed is always lower than the undamped critical speed.

When we include the actions of flexible damped bearings, we find that a situation can exist in which damping causes the critical speed to increase with damping. At high values of damping, the critical speed will approach the Jeffcott critical speed value based on rigid supports.